A Thesis

On

"Study of Microstructural and tribological properties of LM13 Alloy composite foam"

Submitted in the partial fulfillment of requirement for the degree of

Master of Technology

in

Materials & Metallurgical Engineering

by

Amit Sharma

[601202001]

Under the supervision of

Dr. O. P. Pandey
(Senior Professor)

School of Physics and Materials Science

Thapar University, Patiala (Punjab), India.

July-2014

Dedication

This thesis is dedicated to my father **Suraj Sahai Sharma** and my mother **Shiv Devi Sharma** whose inspirations and constant support allowed me to come up to this point and for me they are a symbol of love, trust and greatest personality.

Certificate

This is to certify that this thesis report entitled **"Study of Microstructural and tribological properties of LM13 Alloy composite foam"** which is being submitted by **Amit Sharma** in fulfillment of the requirement for the award of degree of Master of Technology in School of Physics and Materials Science, Thapar University, Patiala, Punjab, India is an exclusive record of candidate's own research under our supervision. The thesis in part or in full has been submitted in any other university or in institute for the award of any degree. The thesis is fit to be considered for the award of degree of Master of Technology.

This is to certify that the above statement made by the candidate is correct and true to best of my knowledge.

Date: 07-07-2014

Place: Patiala

7/7/14

Dr. O.P. Pandey

(Supervisor)
SPMS, Thapar University
Patiala

Countersigned by:

Dr.Kulvir Singh
(Professor & Head)
School of Physics and Materials Science
Thapar University, Patiala,
(Punjab), INDIA

Dr. S.K. Mohapatra
Dean of academic Affairs
Thapar University, Patiala,
(Punjab), INDIA

Acknowledgement

With deep regards and profound respect, I avail this opportunity to express my deep sense of gratitude and indebtedness to **Dr. O. P. Pandey**, Senior Professor, School of Physics and Materials Science, for his keen interest, strong motivation and constant encouragement during the course of the work. He always bestowed parental care upon me and evinced keen interest in solving our problems. An erudite teacher, a magnificent person and a strict disciplinarian, I consider myself fortunate to have worked under his supervision.

I thank him for his great patience, constructive criticism and useful suggestions apart from invaluable guidance to me.

I would also like to thank **Dr. Kulvir Singh**, Professor and Head, School of Physics and Materials Science for his constant guidance and encouragement. I am also thankful to **Dr. Puneet Sharma, Dr. B. N. Chudasama Dr. Dwijendra Pratap Singh, Dr. Manoj Kumar Sharma, Dr. Surendra Deo Tiwari** and all the faculty members of School of Physics and Materials Sciences for their constructive suggestions at different stages of this work.

It gives me immense pleasure to express my special thanks to **Mr. Suresh Kumar** and **Dr. Ranvir Singh Panwar**, who always took keen interest in guiding me during my work.

I am extremely thankful to research scholar **Mr. Gaurav Singla, Mr. Paramjyot Jha, Mr. Mintu Tyagi, and Mr. Sativindar Singh** of Thapar University for constant support. I owe my sincere thanks to all the staff members of School of Physics and Materials Science for their support and encouragement.

I would like to convey my sincere gratitude to my friends and colleagues for their support and their timely help and valuable discussions.

Last but not the least my father **Mr. S. S. Sharma** and my mother **Mrs. S. D. Sharma** are the two guiding pillars of my success, the constant motivation of my parents has been sole source of my inspiration and strength to carry out my work.

Above all, hidden force by **Almighty God** steered me in the right direction to achieve the goal.

Amit Sharma

(AMIT SHARMA)

Abstract

Closed-cell aluminum foam offers a unique combination of properties such as low density, high stiffness, strength and energy absorption that can be tailored through design of the microstructure. With a view, the goal is to develop superior multifunctional properties in the applications such as wear resistance, electrical components and light weight structural parts in industries including aerospace, automotive and defense. In the present investigation, effect of holding temperatures and amount of reinforcement of zircon sand on the microstructure of LM13 alloy foam and LM13 alloy composite foam has been studied. For this purpose LM13 piston alloy of near eutectic composition is used as foaming matrix material and zircon sand particles as reinforcement. Composite foam was developed by stir casting route at different holding temperatures. Variation in microstructures of the composite foam is observed with the addition of zircon sand particles and also with varying holding temperatures. The results show that the microstructural parameters such as cell size, node and ligament increases with increasing holding temperature which affects the tribological properties of cast materials. The wear rates of the samples were measured under dry sliding conditions with different loads. The wear mechanism was investigated and the effects of the foam cell size on the wear properties were determined. Experimental results indicate that reinforcement upto 5% zircon sand enhances the properties like hardness and wear characteristics of the formed foams. Moreover, the cell size and nodes are optimum which is responsible for such a enhanced property.

INDEX

List of Figure

List of Table

Chapter 1
Introduction

Metallic foams and porous metals have attracted lot of interest because of high demand in industries. Porous structures of metal are in demand for applications such as insulation, packaging, or filtering however, apart from these, they can be used as structural materials also [1]. Bone and wood are some examples of natural occurring porous materials. These materials have optimum mechanical properties and structural function with minimum weight. The search for a man made cellular structural material has led to several choices. Metal foams have some excellent properties in comparison to polymers and ceramic materials as polymers are not rigid enough and moreover, ceramic materials are too brittle. Metal foams are stiffer than polymers along with adequate ductility. They are stable at elevated temperatures and possess magnificent fire resistance and are recyclable [2].

Cellular metals and metallic foams are metals with pores intentionally organized in their structure. The terms cellular metals or porous metals referring to metals that have large volume of porosities, while the terms foamed metal or metallic foams applies to porous metals produced with processes where foaming take place. The foaming is the process of introducing gas in any liquid phase. Metal foams are characterized structurally on the basis of shape cells, relative density, cell size, cell shape and anisotropy. Table-1 gives the list of parameters for describing the structure of metallic foams. The structure of closed- pore foams resemble to a network of soap bubbles and can bear high impact loads. The open-pore foams are identical to the closed-cell ones except there are no cell walls present which produce large channels of interconnected cells. Despite the low structural strength of open cell foams flow-through capability is their main advantage [3].

Table-1: List of parameters for describing the structure of metallic foams, based on [4].

<table>
<tr><th colspan="3">Cellular architecture (geometrical structure) = Cells + Cell skeleton of massive metals</th></tr>
<tr><td>• Open or closed cells
• Stochastically or regular arrangement of cells
• Neighborship relation
• Geometrical models (tesselation)</td><td>• Volume fraction
• Aspect ratio
• Orientation
• Size distribution
• Gas content</td><td>• Thickness and length of the cell walls
• Number / area of nodes
• Curvature / corrugation of cell walls
• Chemical composition of cellular material</td></tr>
<tr><th colspan="3">Microstructure</th></tr>
<tr><td>• Dendritic structure
• Grains
• Chemical inhomogeneity
• particles</td><td colspan="2">• Eutectics, eutectic sells
• Micropores
• Inclusions
• Precipitates
• Dislocations
• Surface skin</td></tr>
</table>

Metallic foams have superior combinations of physical and mechanical properties that cannot be achieved with polymer and ceramic foams. Mechanical strength, stiffness and energy absorption of metallic foams are much higher than those of polymer foams. They are thermally and electrically conductive and maintain their mechanical properties at much higher temperatures in comparison to the polymer foams. As opposed to ceramics foams, metallic foams have the ability to deform plastically and absorb a good amount of energy. Low weight and cellular microstructure of metal foams endows them with the ability to absorb energy by plastic dissipation under compression [5]. Open cell metal foams are permeable and can have very high specific surface areas and features required for flow-through applications or when surface exchange are involved. However, most of the mechanical properties of metal foam can be accomplished with other materials, sometimes more effectively, but metal foams can offer a remarkable combination of several properties that cannot be achieved with monolithic formal material at the same time (e.g., ultra-low density, high stiffness, the capability to absorb crash energy, low thermal conductivity, low magnetic permeability, and good vibration damping). Hence, Cellular metals are quite promising in different areas of engineering applications where several of these properties are required to be combined [6].

The main applications of aluminum foams are found in the automotive industry (impact, acoustic and vibration absorbers), the aerospace industry as structural components in turbines and spatial cones, in the naval industry as low frequency vibration absorbers, and in construction industry as sound barriers inside tunnels and as fire proof materials, structure protection systems against explosions and even as decoration. As far as structural applications are concerned, aluminum foams (pure or with the addition of small quantities of other alloying elements) actually represent the most promising typology owing to their mechanical properties at low cost [7, 8].

1.1 Classification of Metallic Foams

The most fundamental classification of metal foams is done on the basis of the degree of interconnection between adjacent cells within the microstructure of the material. Hence metal foams are classified as open and closed cell metal foams.

1.1.1 Open Cell Metal Foam

Open cell metal foams have a wide variety of applications including heat exchangers (compact electronic cooling, cryogen tanks, PCM heat exchangers), energy absorption, flow diffusion and lightweight optics. Due to the high cost of the material it is most typically used in advanced technology, aerospace, and manufacturing. Extremely fine-scale open-cell foams are used as high-temperature filters in the chemical industry.

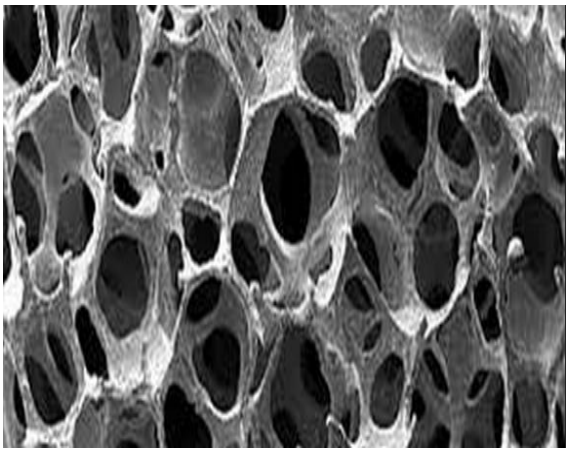

Fig. 1: Macroscopic images of aluminum open cell foam.

Metallic foams are used in the field of compact heat exchangers to increase heat transfer without dropping down the pressure. However, their use permits substantial reduction in the physical size of a heat exchanger, and so fabrication costs. To model these materials, most works uses idealized and periodic structures or averaged macroscopic properties [9].

1.1.2 Closed-Cell Metal Foam

Meller in 1926 firstly reported Closed-cell metal foam in a French patent, where foaming of light metals either by inert gas injection or by blowing agent was suggested [10]. Closed-cell metal foams are primarily used as an impact-absorbing material, similarly to the polymer foams in a helmet but for higher impact loads. In comparison to polymer foams, metal foams remain deformed after impact and can therefore only be used once. They are light and stiff, and are frequently proposed as a lightweight structural material. However, they have not yet been widely used for this purpose.

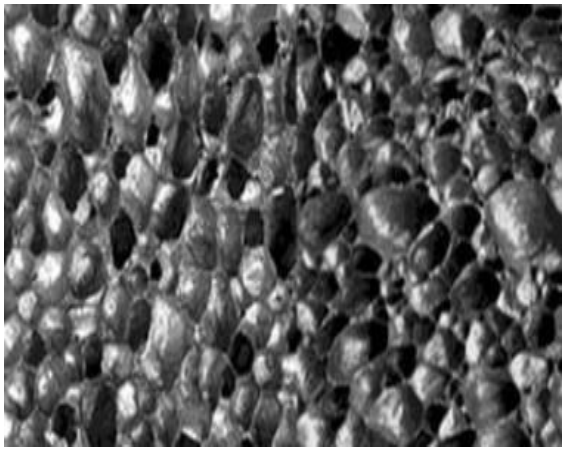

Fig. 2: Macroscopic images of aluminum closed cell foam.

1.2 Metal Foam Production

Metal foams are being made commercially mainly by two processing routes; liquid and solid state processing. In solid state route, powdered metal and powdered titanium hydride or zirconium hydride are mixed, pressed and then heated to melting point of metal to decompose hydride, where hydrogen gas is released which supports the formation of the metal foam.

Alternatively, mixing of slurry of metal powder with foaming agent in an organic adhesive is mechanically charged which after heating endorse porous metal [11].

In liquid state technique, molten metal and stabilizing particulates with foaming agent are mechanically stirred to produce foam. Liquid metals can also be infiltrated around granules which are then removed. Other more sophisticated methods involve electroless, electrochemical or chemical vapor deposition of metal onto an open cell polymer foam. A summary of production methods of foam are given in Table-2.

Table -2: Metal foams production methods based on [12].

Foaming route	**Direct foaming of melt**			**Indirect foaming via remelting of precursor**	
Process name	Alcan/Hydro/ Metcomb	Alporas	Gasar/ Lotus	Alulight/ Fominal	Formgrip
Dominant stabilization factor	Ceramic added to the melt	Oxide formation in melt	Viscosity of eutectic melt	Oxides in compacted powder	Ceramic added to the melt
Gas source	External gas source	Blowing agent	Dissolved gas	Blowing agent	Blowing agent

1.2.1 ALPORAS Process

In ALPORAS process, aluminum foam is made with molten aluminum by stabilizing bubbles in the melt. To stabilize the bubbles, viscosity is increase to prevent the bubbles from floating. In 1967, Ridgway during his work used 1.5 wt.% Ca as a thickening agent [13]. He merged calcium (Ca) with molten aluminum at 680℃ and stirred for 6 min in an ambient atmosphere. The thickened aluminum alloy was poured into a casting mold and stirred with a blowing agent of 1.6 wt.% TiH_2 at 680℃. After stirring, the molten material was aged for about 15 min, which expands and fills up the mold. The foamed molten material is then cooled in the mold with a powerful blower.

1.2.2 FOAMCARP Process

Calcium carbonates based foams are available in the market under the trade name FOAMCARP. Gergely et al. [14] used duraclan type metal (Al-9Si-0.5Mg, with a max. of 0.2 wt.% of Cu, Mg and Ti) with 10 vol.% of SiC particulate is melted in induction furnace at 650℃. After 10 sec of stirring, the foaming agent and Al-12Si powder mixture (1:2 mass ratio) was introduced into the melt and the melt was stirred at approximately 1200 rpm further to get foam. A low porosity precursor block, with a thickness of about 20 mm, was produced by casting the semi-solid composite at room temperature. The amount of incorporated carbonate was 3.5 wt.% of the composite mass. Precursors thus formed were heated upto 750℃ for 15 minutes that lead to thermal decomposition of the foaming agent and the evolved gas (CO_2) foamed the melt.

1.3 Properties of Metal Foams

Metal foam exhibit variable physical and mechanical properties depending upon the nature of pores existing in the system. These physical, mechanical and thermal properties are usually measured by the same methods as those used for dense solids when the variation in properties is observed [15]. The physical properties, such as the heat capacity, are typically linear functions of the density. Even in low density metallic foams the weight fraction of gas is small, so that the specific heat of the cellular structure is essentially equal to that of the parent metal. There are many properties that depend on the density. The geometrical factors also influence the mechanical properties like stiffness and strength. Moreover, the thermal and electrical conductivity as well as acoustic properties depend upon nature of pores. The most important feature of foams is the relative density (ρ_{rel}) that is, the apparent density of the foam (ρ), divided by the bulk density of the material (ρ_0) from which the foam is made [16].

The parameters that influence the structure-sensitive properties of cellular metals are:

- Intrinsic properties (properties of cell wall material),
- Relative density,
- Type of cellular structure (open or closed cells),
- In a closed-cell foam, the fraction of the solid contained in the cell nodes and edges,
- Irregularity or gradients in mass distribution,
- The cell size and size distribution (including exceptional sizes),

- Shape of the cells and the anisotropy of cells (including exceptional shapes),
- Connectivity of cell edges,
- Defects, by which we mean buckled or broken cell walls.

1.3.1 Thermal and Electrical Properties

The conduction of heat in closed-cell metal foams occurs mainly through the solid part of the foam. The contribution of the gas, radiation across the pores, and convection within the cell play a minor role. Therefore, the thermal conductivity of foam should be less than its solid counterpart. The conductivity of the cellular metal should be equal to the conductivity of the dense solid considering the net volume of solid fraction, which is further governed by the geometry. Electrical conduction is also hindered by presence of gas pores and behaves in same manner as that of thermal conductivity.

1.3.2 Mechanical Properties

In contrast to thermal and electrical properties, the influence of the density and the architecture of the cellular metal on the mechanical properties is much stronger and more complex. For load bearing structures, packaging, and for crash element analysis this because more important. However, for other application, like functional applications, for example, heat-exchange systems, damping, and filtering the structural stability is also essential [17]. In compression, cellular metals show a unique stress-strain response with a plateau region in which the stress is nearly constant over a wide range of strain. This behavior makes cellular metals interesting for energy absorbing applications where at a relatively low constant stress a large amount of deformation can be absorbed.

1.3.3 Damping and Sound Absorption

If the structure is subjected to external excitations by sound waves or by mechanical vibrations, the sound can be transmitted or even born by the structure itself. This is most important in the cases, when the structure oscillates at its resonant or eigen frequencies. The amplitude of the structure acoustic response and hence the sound radiation can be dramatically reduced by increasing the damping of the structure. The rate of vibrational dissipation or the damping in the

structure can be characterized by the loss factor. Loss factor depends upon damping capacity of material which can be defined as energy dissipated in a complete cycle. The typical structural materials with high strength (for example steel, cast iron, aluminum alloys) have unfortunately very little damping. On the another hand, the high damping materials, such as lead, rubber, or soft plastic, have little strength and cannot be regarded as structural materials. The cellular metals exhibit at least one order of magnitude higher values of the loss factor. The dissipation of the vibrations mainly results from the friction between the attaching surfaces of the cracks appearing in the structure and partially due to the vibration of the thin pore walls. Thus, the damping can be enhanced by the reduction of the cell-wall thickness or/and by introducing imperfections into the structure. Higher loss factor values are therefore obtained with for example foams made of casting aluminum alloys, which can be prepared with very thin cell walls and contain a lot of cracks. If the consolable ceramic particles, for example SiC, Al_2O_3, or graphite are additionally introduced into the structure of metallic cell walls, the damping will be further improved [17].

For sound absorption purposes highly permeable materials such as open-cell polymer foams and glass or mineral wool fibers are generally used. Flammability and evolution of toxic gases when subjected to excessive heat is the main disadvantage of polymer foams. On the other hand fibrous materials are very sensitive to erosion by shedding or fraying especially under the effects of air flow or vibration. Both types of absorbers usually require various facing materials in order to improve durability or to protect the absorber from contamination. Accordingly, the main parameter for good sound absorption is the permeability of the absorber. Therefore, cellular metals can be used for this purpose only if they meet this fundamental requirement. The closed-cell metallic foams are too stiff to convert sound energy into heat by vibration of their cell walls. To increase the sound absorption of closed-cell foams can be machined that result in rough open-pore surface that slightly improves the sound absorption.

1.3.4 Behavior Under Compressive Loading

The compression load deflection curve of aluminum foam can be divided into three different regions. At low deflection the material deforms almost elastically (cell walls bend), then a plateau of deformation at approximately constant load exists (cell walls buckle, yield or fracture) and finally there is a region of rapidly increasing load after the cell walls crushed together. For

the load at the beginning of the second part of the load-deflection curve (plateau), i.e. when significant plastic deformation starts, a stress can be calculated and defined as a plastic collapse stress or as compression strength.

Plastic collapse stress increases with increasing density significantly. It can be improved by appropriate heat treatment. The collapse mode for aluminum foam i.e. buckling or breaking of the cell walls can be influenced by the composition of the base alloy or by the thermal treatment of the foamed part. Foams based on cast aluminum alloys (e.g. Al-12Si) tend to the breaking of the cell walls, the wrought alloys tend to the bending and buckling of the cell walls.

The area under the load-deflection curve illustrates the energy needed for plastic deformation. The energy used for plastic deformation until the given load is applied on the foam is very important parameter if the impact energy absorption is considered. Also this energy depends strongly on the apparent density. If the density is too low the foam crushes before impact energy is sufficiently absorbed. If the density is too high the stress in the foam exceeds the given critical value at low absorbed energy.

1.3.5 Electromagnetic Shielding

Electromagnetic wave shielding is used to protect electronic devices and room interiors from the negative influence of electromagnetic waves. The ability to reflect the electromagnetic energy can be defined by the shield effectiveness.

1.3.6 Gamma Rays Shielding

Developing new multifunctional materials in recent years for nuclear systems has become increasingly critical owing to the high demand on better shielding in extreme environments. Radiation shielding materials and components of shielding structures should possess good mechanical properties, long-term reliability, good fabrication and joining properties with suitable thermo-physical characteristics [18]. Particular emphasis must be given to low density, high radiation tolerance and energy absorption capabilities due to new mission criteria in nuclear industries. Summary of some potential applications of metals foams are tabulated below:

Table-3: Potential application for metal foams, based on [19].

Application	Comments	Examples
Light weight structures	Excellent stiffness to weight ratio when loaded in bending.	Shipping container, building material, filling in hallow material against buckling and builders staging.
Sandwich cores	Metal foams ha low density with good shear and fracture strength.	Panel like floor and drop ceiling, aircraft pallet, heavy duty pallet, panels replacing honeycomb, elevator cab and door.
Strain isolation (compression)	Metal foams can take up strain mismatch by crushing at controlled pressure.	Joining elements
Mechanical damping	The damping capacity of metal foams is larger, by up to a factor of 10, than that of solid metals.	Basis of rotating machine or loudspeaker
Acoustic absorption	Open cell foam have sound absorbing capacity.	Sound barrier for highways, overhead bridge and tunnel, machine casing with improved sound and vibration damping.
Kinetic energy absorbers (compressive)	Exceptional ability to absorb energy at almost constant pressure	Crash attenuator, crash barrier, safety wall of tornado shelter, crash helmet, impact energy absorption parts for cars, lifting and conveying system.
Blast resistance	Excellent energy absorption capability.	Amour and gas tank
Artificial wood (with high temperature capability)	Metal foams has some wood-like characteristics: light, stiff and ability to be joined with wood screw	Rail car bulkhead, fire door and wall.
Heat exchangers / refrigerators	Open cell foams have large accessible surface area and high cell	Heat sink for processors

	wall conduction giving exceptional heat transfer ability.	
Thermal isolation	Thermal conductivities are much lower than those of solid metals, but still much larger than polymer foam.	Cooking pot and vessels
Heat shields	Oxidation of cell faces of closed-cell aluminum foam appears to impart exceptional resistance to direct flame.	Fireproof wall
Electrodes shielding	Good electrical conduction, mechanical strength and low density make metal foams attractive for shielding.	Housings for electronic devices providing electromagnetic and thermal shielding
Electrodes and catalyst carriers	High surface / volume ratio allows compact electrodes with reaction surface area.	Long life battery
Buoyancy	Low density and good corrosion resistance suggest possible flotation application.	Ship and boat

REFERENCES

[1] H. P Degischer, and B Kriszt, "Handbook of Cellular Metals, Production, Processing, Applications", (2002).

[2] Louis-Philippe Lefebvre, John Banhart and David C. Dunand, "Porous metals and metallic foams: Current status and recent developments". Advanced Engineering Materials. Vol-10, pp.775-787, (2008).

[3] Amol A. Gokhale, N.V. Ravi Kumar, B. Sudhakar, S. N. Sahu, Himalay Basumatary, and S. Dhara, "Cellular metals and ceramics for defence applications". Defence Science Journal. Vol-61, pp.567-575, (2001).

[4] B. kriszt, U. Martin and U. Mosler, "Characterization of cellular and foamed metals, ch.4.1, in Handbook of cellular metals". (Ed.: H.P. Degischer and B.Kriszt), WILEY VCH, Weinheim, pp.130-145, (2002).

[5] L.J. Gibson and M.F. Ashby, "Cellular solids: structure and properties". (1997).

[6] M.F. Ashby, A.G. Evans, N.A. Fleck, L.J. Gibson, J.W. Hutchinson and H.N.G. Wadley, "Metal Foams: A design guide". Butterworth-Heinemann. (2000).

[7] H.P. Degischer and B. Kriszt, "Handbook of cellular metals: Production, processing, applications". Wiley-VCH Verlag GmbH & Co. KGaA. (2002).

[8] Roberto Montanini, "Measurement of strain rate sensitivity of aluminum foams for energy dissipation". International Journal of Mechanical Sciences. Vol-47, pp.26-42. (2005).

[9] R. Rajendran, K.P. Sai, B. Chandrasekar, A. Gokhale, and S. Basu, "Materials and Design". Vol-29, pp.1732–739. (2008).

[10] De Melle, "French Patent FR000000615147A". Dec. 30, (1926).

[11] V. Gergely, H.P. Degischer and T.W. Clyne, "Recycling of MMCs and production of metallic foams, Comprehensive Composite Materials". Vol-3, pp.797-820, (2000).

[12] J. A. Ridgway Jr., "US Patent 3" pp.297-431, (1967).

[13] H.P. Degischer and B. Kriszt, "Handbook of cellular metals: Production, processing, applications". (2002).

[14] S Das, V. Udhayabanu S. Das, and K. Das, "Synthesis and characterization of zircon sand/Al-4.5 wt% Cu composite produced by stir casting route". Jouneral of Mater Science. Vol-41, pp.4668-4677, (2006).

[15] Reimund Neugebauer, Thomas Hipke, Jorg Hohlfeld, and Rocco Thummler, "Highly damped machine tools with metal foam". Advanced metallic materials. pp.214-218. (2003).

[16] J.T Busby, K.J Leonard, "JOM Journal of the Minerals Metals and Materials Society". Vol-59, pp.20-26, (2007).

[17] M.F. Ashby, A. G. Evans, J. W. Hutchinson and N. A. Fleck, "Metal Foams: a Design Guide". Butterworth-Heinemann. ISBN 0-7506-7219-6, (2000).

Chapter 2

Literature Review

This chapter contains the study of work done by the different researcher on the development of aluminum foam. However, the emphasis is given on recent work to tune our work with recent development.

Frantisek et al. in 1997 [1] studied the isotropic properties of metallic aluminum foams with a cellular structure. They suggested that essentially spherical and closed pores occupy more than 70% of the total volume. Mechanical and physical properties depend strongly on the density which lies typically in the range of 0.4-1.2 g/cm^3. They also reported that aluminum foam prepared by powder metallurgical method is very efficient in sound absorption, electromagnetic shielding, impact energy absorption and vibration damping.

Banhart et al. in 1998 [2] proposed that under uniaxial compression the stress-strain diagram of metal foam depends on the density of the foam, the relative orientation of the testing and foaming direction, and also on the orientation of closed outer skins. They found that higher densities in general lead to higher stresses under compression conditions but also to a reduction of the range of the technologically important plateau regime. A parallel orientation of the outer skins with respect to the applied force leads to a higher strength with an extension of the plateau regime as compared to the perpendicular orientation. The relative orientation of force and foaming direction, however, is of minor importance. They found that foams investigated were therefore nearly isotropic. The observed influence of closed and densified outer skins was comparable to the behavior of foams with a high plateau stress.

McCullough et al. in 1999 [3] developed the anisotropic foams, markedly inhomogeneous and have properties close to those expected of an open cell foam. The modulus and the tensile and compressive yield strength was increased non-linearly with relative density. They analyzed deformation mechanisms using image analysis software and a d.c. potential drop technique. The tensile and compressive stress strain behavior of closed cell aluminum alloy foams was measured and interpreted in terms of its microstructure. These include non-uniform density, weak oxide

interfaces, and cell faces containing voids and cracks. The scatter in results was attributed to imperfections within the foam in their work.

Gergely et al. in 1999 [4] reported the stability of the liquid metallic foams during preparation of aluminum foam. In their work, the fabrication route involves infiltration of the spaces between ceramic layers with expanding semi-liquid metal foam. Examination of the foam macrostructure revealed that cell coarsening is very sensitive to the foam baking parameters (temperature and time). Theoretical analysis of material redistribution in the liquid foam showed that foam stability can be improved by increasing the melt viscosity. However, analysis suggests that the size of particles should be kept reasonably small because the "life time" of small cells was significantly reduced when the particles are larger.

Miyoshi et al. in 2000 [5] worked on ALPORAS, which is closed-cell type aluminum foam and was manufactured by batch casting in which Al is thickened by Ca and blown by TiH_2. The density of the general type foam was 0.18 ± 0.24 g/cm^3 and its mean cell diameter was 4.5 mm. Excellent sound absorption and shock absorption capabilities of the foam was reported.

Yang et al. in 2000 [6] examined the factors which affect the foaming in a foamed aluminum casting process. They proposed that proper controlling holding temperature and titanium hydride content of the melt lead to the production of foamed aluminum, which contains uniform cell structure of high porosity. By addition of 1% titanium hydride at 640 ^{0}C, an optimum foamed aluminum was obtained with air bubbles of 2 to 6 mm diameter and a uniform distribution with 86% porosity.

Stanzick et al. in 2000 [7] mentioned that metal foams can be produced in different ways. The investigation of the actual evolution process is always difficult owing to the specific properties of metallic melts. The presents work two types of in-situ observations of expanding and decaying metal foams: firstly the measurements of the time dependent volume as the foam evolved and second, observations of the internal bubble structure by X-ray radiography. For the former experiment a specially constructed dilatometer was used which allows for a controlled expansion of the metallic melt while measuring its volume and temperature.

Zitha et al. in 2001 [8] developed the technique to study the foaming with variable molten metals with viscosities. Such melts could be foamed by injecting gases or by adding gas-releasing blowing agents which caused the formation of bubbles during in-situ decomposition. A further way was to prepare supersaturated metal-gas systems under high pressure and initiate

bubble formation by pressure and temperature control. The powder mixtures along with blowing agent were compacted and the mixture was then foamed by melting. The various foaming processes, the foam stabilizing mechanisms and the existing problems with the various methods were addressed.

Banhart in 2001 [9] in his work classified the various manufacturing processes according to the state of matter in which the metal was processed as solid, liquid, gaseous or ionized. Liquid metal could be foamed directly by injecting gas or gas-releasing blowing agents, or by producing supersaturated metal–gas solutions. Indirect methods included investment casting, the use of space holding filler materials or melting of powder compacts, which contained a blowing agent. If inert gas was entrapped in powder compacts, a subsequent heat treatment could produce cellular metals even in the solid state. Finally, metal vapor deposition also allowed for the production of highly porous metallic structures. The various application fields for cellular metals were discussed. These were divided into structural and functional applications and were treated according to their relevance for the different industrial sectors.

Kovacik et al. in 2001 [10] in their work measured the electrical conductivity of Al and Zn based foams prepared by powder metallurgical route with the porosity in the range of 60-90% and modeled by means of percolation theory. It is shown that electrical conductivity of metallic foams depend predominantly on the electrical conductivity of the matrix metal or alloy and the foam density. It was revealed that the simplified percolation model describes fairly well conductivity-porosity relationship. However, the characteristic exponents obtained experimentally was found lower than the theoretically predicted value due to the effect of sample size, surface skin, heterogeneity of foam structure, and the setting of the percolation threshold to zero. The effects of surface skin, heterogeneity of the structure and sample size were further demonstrated.

Simancik et al. in 2001 [11] proposed that the aluminum foams prepared by PM-techniques were very promising materials for lightweight stiff body structures and crash absorbing elements. However, their surface skin usually contained small holes or even cracks which could initiate premature fracture of the foam, especially when they appeared on the tensile loaded surface. Strengthening of surface skin with various reinforcements could solve this problem very effectively. According to a novel foaming technique, the reinforcements were placed in the foaming mold together with foamable precursor and in a course of foam expansion they were

infiltrated with molten cell-wall material. The main advantage of this method was the simplicity, lower manufacturing costs and the possibility to reinforce the foamed part selectively and anisotropically according to the applied load.

Hashim et al. in 2002 [12] proposed that processing variables such as holding temperature, stirring speed, size of the impeller, and the position of the impeller in the melt were among the important factors to be considered to improve the mechanical properties. The level of the intimate contact of the wetting element with the matrix materials, and also the porosity content are the influencing factor. Therefore, by controlling the processing conditions as well as the relative amount of the reinforcement material, it was possible to obtain a composite with a broad range of mechanical properties. The method was potentially cost effective, but widespread adoption was dependent on a satisfactory resolution of the technical difficulties presented.

Gregely et al. in 2003 [13] presented a brief outline of the factors that were involved in the search for gas generating agents offering superior performance for foaming of liquid aluminum alloys. These included kinetic and thermodynamic characteristics of decomposition reactions, the ease of dispersion of the powdered foaming agent in the melt, the nature and likely effect of decomposition products on melt flow, potential reactions, cost and ease of handling of the powder concerned. Calcium carbonate as foaming agent offered advantage are as compared to currently-employed hydride powders in virtually all aspects of their performance. They found that foams could be produced having appreciably finer cells (<1 mm diameter) and more uniform cell structures than currently available melt route foams, a potentially lower ceramic content in the cell walls dramatically reduced raw material costs. The presence of an oxidizing foaming gas in the cells led to reaction with the liquid cell surface, forming a continuous oxide film. The presence of this film had a significant effect on foam stabilization, slowing down cell coalescence and melt drainage.

Heflen et al. in 2005 [14] used Synchrotron-radiation tomography to investigate early foaming stages of aluminum alloys. Monochromatic radiation, high spatial resolution down to the micrometer scale, partial beam coherence, and holographic reconstruction techniques permitted the distinction between different foam constituents which were not visible by other volume imaging techniques. In combination with three-dimensional image analysis, the differences in the pore initiation processes in two different aluminum alloys were shown. It was found that, in powder compacts made from pre-alloyed AA6061 alloy powder, pores appeared predominantly

around the blowing agent particles whereas, in compacts made from a powder blend of Al and Si, pores tend to initiate around Si particles.

Montanini et al. in 2005 [15] investigated the structural performance of aluminum alloy foams under both static and dynamic compression loads. Three categories of foams (M-PORE, CYMAT, SCHUNK) in a wide range of density (from 0.14 to 0.75 g/cm^3), made by means of different process-routes (melt gas injection, powder metallurgy, investment casting) were analyzed. Microstructure was obtained by SEM and Computed Tomography (CT) and subsequently digital image processing in order to determine average cells size and cell distributions on different section planes. The experimental study aimed to assess the mechanical behavior and the physical and geometrical properties of the foam. They found that the specific energy dissipation of foams with similar density can be quite different: for the same volume of foam, average values of 1770, 1780 and 5590 J/kg at 50% nominal compression have been measured on M-PORE (0.19g/cm^3), CYMAT (0.28g/cm^3) and SCHUNK (0.28g/cm^3) foams, respectively. Impact tests showed that the dependence of the plateau stress on strain rate could be considered negligible for M-PORE and CYMAT foams while it is quite remarkable for SCHUNK foams. Moreover, it was found that the peak stress of CYMAT foams has a quite large sensitivity on the loading rate.

Bryant et al. in 2006 [16] described an alternative processing method for producing aluminum foams. They found that the physical and mechanical properties in these fine (< 1 mm) celled aluminum foams was related to their cellular structure and the properties of the aluminum alloy matrix from which they were produced. Analysis of these materials showed that foam products can be produced over a range of relative densities (7 to 30%) and that average cell diameters can be refined to values of less than 0.5 mm, allowing for the use of the material in thin panel applications. Density of the foam dominates the strength and modulus of the product, following the power law relationship for open cell structures. This relationship breaks down, however, at low densities where the meso-structure and interconnectivity play a more significant role.

Tzeng et al. in 2007 [17] proposed a modified technique for manufacturing closed-cell aluminum (Al) foams to reduce the cost. The addition of foaming agents promotes the uniformity of cell sizes and controls the viscosity of the melting aluminum alloy. This work elucidated the mechanical characteristics of closed-cell aluminum foams under compressive loading. The thermal conductivity of the aluminum foams was determined and compared with some

theoretical predictions. The optimum parameters for meeting some practical design requirements, such as impact absorption and thermal insulation design applications, were discussed. Finally, an empirical correlation between the normalized yield strength and the relative densities was obtained.

Banhart et al. in 2008 [18] manufactured sandwich panels consisting of a highly porous aluminum foam core and aluminum alloy face sheets by roll-bonding aluminum alloy sheets to a densified mixture of metal powders, usually Al-Si or Al-Si-Cu alloys with 6-8% Si and 3-10% Cu and titanium hydride, and foaming the resulting three-layer structure by a thermal treatment. Various processing steps of aluminum foam sandwich (AFS), the metallurgical processes during foaming and alternative ways to manufacture AFS (e.g. by adhesive bonding) was reviewed. AFS can be treated in two ways after foaming i.e. forging and age-hardening.

Dudka et al. in 2008 [19] worked on foaming of aluminum under oxidising and non-oxidising gas atmospheres. They prepared the metal foam by mixing and pressing Al99.95 and TiH_2 powders and foaming the pressed material in a gas-tight X-ray transparent furnace while following the process by X-ray radioscopy. Structure and distribution of the oxides present in the powders, precursors and foams were studied by light microscopy, scanning and transmission electron microscopy. Sequential focused ion beam slicing was used to obtain tomographic images of oxide and micro-pore distributions within the individual cell walls of the foams. A complex hierarchical structure of the oxides was found. Oxides reside in the bulk of the cell walls without a pronounced segregation to the gas/metal interfaces. The presence of air retards foaming due to oxidation of the outer surface.

Cambroneroa et al. 2009 [20] Used two calcium carbonate powders as foaming agents on an Al-Mg-Si (AA6061) alloy in their study. Their different characteristics (particle size and chemical composition) modified the manufacturing process to achieve the final foam. AA6061 powders were then mixed with 10% calcium carbonate and, after cold isostatic pressing into green cylinders, hot extruded at different temperatures (475-545°C). The foaming treatment was carried out in a furnace preheated to 750°C using several heating times. The density changed from 2.03 to 2.10 g/cm^3 after cold isostatic pressing to 2.64–2.69 g/cm^3 in precursor materials obtained by hot extrusion. Foaming behavior depends on the carbonate powder as well as the extrusion temperature. Thus, natural carbonate powder (white marble) produces a foam density close to 0.65 g/cm^3 after a shorter time than when chemical carbonate is used. The foam structure

showed a low degree of aluminum draining with no wall cell cracking and a good fine cell size distribution. Compressive strength of 6.11 MPa and 1.8 kJ/m^3 of energy absorption were obtained on AA6061 foams with a density between 0.53 and 0.56 g/cm^3.

Solorzano et al. in 2009 [21] proposed a novel method for measuring the temperature distribution and evolution of metal foams in the molten state. Foamable AlSi9 precursor material containing 0.6 wt.% TiH_2 was foamed, kept at high temperatures and solidified while its temperature distribution was monitored by a thermographic camera. Free foaming and foaming inside a closed mold were carried out and direct and screened IR monitoring were done. Different heating conditions were applied giving rise to homogeneous and inhomogeneous temperature distributions. The effect of oxidation was studied on a piece of pure aluminum for reference purposes. The error sources of the measured temperature were analyzed. Direct monitoring of foams was shown to be associated to serious problems with quantitative temperature measurement, while screened monitoring yielded promising and accurate quantitative results.

Haesche et al. 2010 [22] investigated replacement of TiH_2 as foaming agent by $CaCO_3$ (lime) and $CaMg(CO_3)_2$ (dolomite) for AlMg4.5 and AlSi9Cu3 foams considering influences on foaming capability and cellular structure. Precursor materials were produced from alloy chip and powder mixtures by means of the thixocasting process. AlSi9Cu3 variants showed expansion levels sufficient for commercial use. Improved performance of dolomite-based foams relies on formation of stabilizing MgO phases, which do not develop during decomposition of $CaCO_3$ in Al-Si-Cu alloys.

Mukherjee et al. in 2010 [23] studied the application of different cooling rates as a strategy to enhance the structure of aluminum foams. The potential to influence the level of morphological defects and cell size non-uniformities is investigated. AlSi6Cu4 alloy was foamed through the powder compact route and then solidified applying three different cooling rates. Foam development was monitored in-situ by means of X-ray radioscopy while foaming inside a closed mold. The macrostructure of the foams was analyzed in terms of cell size distribution as determined by X-ray tomography. Compression tests were conducted to assess the mechanical performance of the foams and measured the properties. Further they correlated the structural features of the foams. Moreover, possible changes in the ductile-brittle nature of deformation with cooling rate were analyzed by studying the initial stages of deformation. Improvements in

the cell size distributions, reduction in micro-porosity and grain size at higher cooling rates was observed, which in turn led to a notable enhancement in compressive strength.

Malekjafarian et al. in 2012 [24] manufactured foamy Al alloy SiCp composites of different densities ranging from 0.4 to 0.7 g/cm^3 by melt-foaming process, which consisted of direct $CaCO_3$ addition into the molten A356 aluminum bath. Mechanical properties and morphological observations indicated that the three-stage deformation mechanism of typical cellular foams is dominant in the produced A356 aluminum foams. Middle-stage stress plateau shrinkage plus compressive strength and bending stress enhancements were observed in denser foams. With the same Al/SiCp ratio, energy absorption ability and plastic collapse strength of the closed-cell foams were increased with the foam density. Doubling cell-face bending effects resulted in larger compressive than bending strengths in the closed-cell foams while laver stiffness was due to the cell-face stretching conditions.

Iluk in 2012 [25] investigated the behavior of standalone absorber made of ALPORAS aluminum foam. The limiting parameters in the given foam component are the stability of absorber column and the risk of global buckling. Specimens with different slenderness ratio were crushed in order to find the transition point between local collapse of the cell walls and global buckling of the entire column.

Cree et al. in 2011 [26] in their study observed the dry sliding wear and friction behaviors of A356 aluminum alloy and a hybrid composite of A356 aluminum alloy and silicon carbide foam in the form of an interpenetrating phase composite were evaluated using a ball-on-disk apparatus at ambient conditions. The stationary 6.35 mm alumina ball produced a wear track (scar) diameter of 7 mm on the rotating specimen surface. Three different loads; 5 N, 10 N and 20 N were applied at a constant sliding speed of 33 mm/s for both materials. Wear tracks were characterized with a scanning electron microscope and measured with an optical surface profilometer. In general, this novel A356/SiC foam composite reduced the friction coefficient and wear rate from that of the base alloy for all loading conditions. In addition, as the load increased, the friction coefficient and wear rate decreased for both materials. The results indicate the composite could be used in light-weight applications where moderate strength and wear properties are needed.

Jha et al. in 2011 [27] in their study observed the sliding wear behavior of cenosphere-filled aluminum syntactic foam (ASF) and composed it with that of 10 wt% SiC particle reinforced

aluminum matrix composite (AMC) at a load of 3 kg with varying sliding speeds under dry and lubricated conditions using a pin-on-disc test apparatus. The tribological responses such as the wear rate, the coefficient to friction and the frictional heating were investigated. The wear surface sand subsurfaces were studied for understanding the wear mechanism. It was noted that the coefficient of friction, the wear rate, and the temperature rise for ASF are less than that for AMC in both dry and lubricated conditions. The craters (vis-à-vis exposed cenospheres) play an important role in the wear mechanism for ASF.

Vesenjak et al. in 2012 [28] reported the behavior of metallic foam under impact loading and shockwave propagation. The main goal of their work was to investigate the material and structural properties of submerged open-cell aluminum foam under impact loading conditions with particular interest in shock wave propagation and its effects on cellular material deformation. For this purpose experimental tests and dynamic computational simulations of aluminum foam specimens inside a water tank subjected to explosive charge have been performed. Comparison of the results shows a good correlation between the experimental and simulation results. The shadowgraph method was used to observe the underwater shock wave formation, propagation and its effect on submerged aluminum foam sample. The average shock wave velocity was determined to be approximately 2,700 m/s. The deformation behavior of submerged aluminum foam sample was not studied in detail due to insufficient imaging resolution used in experimental testing.

Byakova et al. in 2012 [29] highlighted the role of foaming agent and processing route influencing the contamination of cell wall material by side products, which, in turn, affect the macroscopic mechanical response of closed-cell Al-foams. Several kinds of Al-foams have been produced with pure Al by the ALPORAS melt process and powder metallurgical technique, all performed either with conventional TiH_2 foaming agent or $CaCO_3$ as an alternative. Mechanical characteristics of contaminating products induced by processing additives, all of which were presented in one or another kind of Al-foam, have been determined in indentation experiments. Damage behavior of these contaminations affects the micro-mechanism of deformation and favors either plastic buckling or brittle failure of the cell walls.

Koizumi et al. in 2012 [30] observed the cell structures to study the shrinkage of aluminum foam produced using carbonates. The cells of foam produced by using dolomite as a foaming agent connected to each other with maximum expansion. It was estimated that foaming gas was

released through connected cells to the outside. It was assumed that cell formation at different sites is effective in preventing shrinkage induced by cell connection. The multiple additions of dolomite and magnesium carbonate, which have different decomposition temperatures, were applied. The foam in the case with multiple additions maintained a density of 0.66 up to 700°C, at which the foam produced using dolomite shrank. It was verified that the multiple additions of carbonates are effective in preventing shrinkage.

Garcia-Moreno et al. 2012 [31] reviewed the use of X-ray radioscopy for in-situ studies of metal foam formation and evolution. Results demonstrated the power of X-ray radioscopy as diagnostic tool for metal foaming. Qualitative analyses of foam nucleation and evolution, drainage development, issues of thermal contact, mold filling, cell wall rupture have been done. Additionally, quantitative analyses based on series of images of foam expansion yielding coalescence rates, density distributions, etc., were performed by dedicated software. These techniques help to understand the foaming behavior of metals and to improve both foaming methods and foam quality.

Goel et al. in 2013 [32] developed closed cell aluminum fly ash foam through liquid metallurgy route. They investigated its stress-strain behavior at different strain rates ranging from 700 s^{-1} to 1950 s^{-1}. The numerical model of split Hopkinson pressure bar (SHPB) was simulated using commercially available finite element code Abaqus/Explicit. Validation of numerical simulation was carried out using available experimental and numerical results. Full scale stress strain curves were developed for various strain rates to study the effect of strain rate on compressive strength and energy absorption. The results showed that the closed cell aluminum fly ash foam is sensitive to strain rate.

Kamm et al. 2013 [33] investigated different hydrides that could replace TiH_2 as the most suitable blowing agent for foaming aluminum alloys. Hydrides taken from the group MBH_4 (M=Li, Na, K) and $LiAlH_4$ were selected. Foamable precursors of alloy $AlSi_8Mg_4$ were manufactured by pressing blends of metal and blowing agent powders. Powders, precursors and precursor filings were studied by mass spectrometry to obtain the hydrogen desorption profile. Foaming experiments were conducted with simultaneous X-ray radiographic. Two Li-containing blowing agents were found to perform well and can be considered alternatives to TiH_2.

Xia et al. in 2013 [34] prepared closed-cell AZ31-Mg alloy foams by melt-foaming method. Homogenizing heat treatment was applied on the foams and the effects of heat treatment on

compressive properties of closed-cell Mg alloy foams were investigated systematically. The results showed that homogenizing heat treatment enhanced the compressive properties in terms of yield strength, mean plateau strength, available energy absorption capacity and ideality energy absorption efficiency of the foams. In addition, homogenizing heat treatment greatly reduced the stress drop rates of the foams. Specimens homogenized at the temperature of 480°C for 24 h possessed good combination of yield strength, compressive stability, available energy absorption capacity and ideality energy absorption efficiency under the present experimental conditions.

Mondal et al. in 2014 [35] prepared closed-cell zinc aluminum alloy (ZA27)-SiC composite foam which was synthesized using conventional stir-casting technique and CaH_2 as foaming agent. The synthesized foams are characterized in terms of its micro-architectural characteristics and deformation responses under compressive loading. It is observed that ZA27-SiC foams could be easily foamed without any difficulty. The density of the developed foam ranges from 0.25 gm/cc to 0.45 gm/cc due to the variation of CaH_2 percentage. The plateau stress and energy absorption of these foams follow power law relationship with relative density. Wherein, the densification strain follows a linear relationship with the relative density.

REFERENCES

[1] F. Simaneik, J. Jerz, J. Kovaeik, and P. Minar, "J. Metallic Materials". Vol-35(4), pp.265-277, (1997).

[2] J. Banhart and J. Baumeister, "Journal of Materials Science". Vol-33, pp.1431, (1998).

[3] K.Y.G. McCullough, N.A. Fleck and M.F. Ashby, "Uniaxial Stress Strain Behavior of Aluminum Alloy Foams". Acta Materialia. Vol-47, pp.2323-2330, (1999).

[4] V. Gergely, F.Simancík, T. J. Matthams, and T. W. Clyne, "12th Int. Conf. on Composite Materials, Paris". pp.589, (1999).

[5] Tetsuji Miyoshi, Masao Itoh, Shigeru Akiyama, and Akira Kitahara, "Advanced Engineering Materials". Vol-2, pp.179-183, (2000).

[6] C.C. Yanga, and H. Nakae, "Journal of Alloys and Compounds". Vol-313, pp.188-191, (2000).

[7] Heiko Stanzick, John Banhart, Lukas Helfen, and Tilo Baumbach, "Applied. Physic Letter". Vol-78, pp.1152, (2001).

[8] P. Zitha, J. Banhart, and G. Verbist, "MIT-Verlag Bremen". pp.13-20, (2000).

[9] John Banhart, "Progress in Materials Science". Vol-46, pp.559-632, (2001).

[10] J. Kovacik, S. Barta, and J. Bielek, "In advanced metallic materials, Bratislava IMMM SAS". pp.55-58, (2003).

[11] F. Simaneik, Luean, and J.Jerz, "MIT-Verlag". pp.1-6, (2001).

[12] J. Hashim, L. Looney and M.S.J. Hashmi, "Particle distribution in cast metal matrix composites". Journal of materials processing & technology. Vol-123, pp.251-257, (2002).

[13] V. Gergely, D.C. Curran, and T.W. Clyne, "The FOAMCARP process: foaming of aluminum MMCs by the chalk-aluminum reaction in precursors". Composites Science and Technology. Vol-63(16), pp.2301-2310, (2003).

[14] L. Helfen, T. Baumbach, P. Cloetens, P. Pernot, H. Stanzick, K. Schladitz and J. Banhart, "Investigation of pore initiation in metal foams by synchrotron-radiation tomography". Applied Physics Letters. Vol-86, pp.231907, (2005).

[15] Roberto Montanini, "Measurement of strain rate sensitivity of aluminum foams for energy Dissipation". International Journal of Mechanical Sciences. Vol-47, pp.26-42, (2005).

[16] J. Daniel Bryant, Deborah Wilhelmy, Jacob Kallivayalil and Wei Wang, "Development of aluminum foam processes and products". Materials Science Forum. vol-521, pp.1193-1200, (2006).

[17] Sheng-Chung Tzeng and Wei-Ping Ma, "A novel approach to the manufacturing and experimental investigation of closed-cell Al foams". The International Journal of Advanced Manufacturing Technology. Vol-32, pp.473-479, (2007).

[18] John Banhart, and Hans-Wolfgang Seeliger, "Aluminum foam sandwich panels: Manufacture, metallurgy and applications". Advanced Engineering Materials. Vol-10, pp.793-802, (2008).

[19] Alexander Dudka, Francisco Garcia-Moreno, Nelia Wanderka and John Banhart, "Structure and distribution of oxides in aluminum foam". Acta Materialia. Vol-56, pp.3990-4001, (2008).

[20] L.E.G. Cambroneroa, J.M. Ruiz-Romana, F.A. Corpasb and J.M. Ruiz Prieto, "Manufacturing of Al-Mg-Si alloy foam using calcium carbonate as foaming agent". Journal of Materials Processing Technology. Vol-209, pp.1803-1809, (2009).

[21] E. Solorzano, F. Garcia-Moreno, N. Babcsan and J. Banhart, "Thermographic monitoring of aluminum foaming process". Journal of Nondestructive Evaluation. Vol-28.3-4, pp.141-148, (2009).

[22] Marco Haesche, Dirk Lehmhus, Jorg Weise, Manfred Wichmann and Irene Cristina Magnabosco Mocellin, "Carbonates as foaming agent in chip-based aluminum foam precursor". Journal of Material Science and Technology. Vol-26, pp.845-850, (2010).

[23] M. Mukherjee, F. Garcia-Moreno and J. Banhart, "Solidification of metal foams". Acta Materialia. Vol-58, pp.6358-6370, (2010).

[24] M. Malekjafarian and S.K. Sadrnezhaad, "Closed-cell Al alloy composite foams: Production and characterization". Materials and Design. Vol-42, pp.8-12, (2012).

[25] A. Iluk, "Global stability of an aluminum foam stand-alone energy absorber". Archives of civil and mechanical engineering. Vol-13, pp.137-143, (2012).

[26] D. Cree, and M. Pugh, "Dry wear and friction properties of an A356/SiC foam interpenetrating phase composite". Wear. Vol-272, pp.88-96, (2011).

[27] Nidhi Jha, Anshul Badkul, D.P.Mondal, S.Das, and M.Singh, "Sliding wear behaviour of aluminum syntactic foam: A comparison with Al–10 wt% SiC composites". Tribology International. Vol-44, pp.220-231, (2011).

[28] Matej Vesenjak, Matej Borovinsek, Zoran Ren, Seiichi Irie and Shigeru Itoh, "Behavior of metallic foam under shock wave loading". Metals. Vol-2, pp.258-264. (2012).

[29] Alexandra Byakova, Svyatoslav Gnyloskurenko and Takashi Nakamura, "The role of foaming agent and processing route in the mechanical performance of fabricated aluminum foams". Metals. vol-2, pp.95-112, (2012).

[30]. Takuya Koizumi, Kota Kido, Kazuhiko Kita, Koichi Mikado, Svyatoslav Gnyloskurenko, and Takashi Nakamura, "Method of preventing shrinkage of aluminum foam using carbonates". Metals. Vol-2, pp.1-9, (2012).

[31]. Francisco Garcia-Moreno, Manas Mukherjee, Catalina Jimenez, Alexander Rack and John Banhart, "Metal foaming investigated by x-ray radioscopy". Metals. Vol-2, pp.10-21, (2012).

[32] Manmohan Dass Goel, Vasant A. Matsagar, Anil K. Gupta and Steffen Marburg, "Strain rate sensitivity of closed cell aluminum fly ash foam". Transaction of Nonferrous Meterials Society China. Vol-23, pp.1080-1089, (2013).

[33] Paul H. Kamm, F. Garcia-Moreno, Catalina Jimenez and J. Banhart, "Suitability of various complex hydrides for foaming aluminum alloys". Journal of Materials Research. Vol-8, pp.2044-5326, (2013).

[34] Xingchuan Xia, Weimin Zhao, Xiangzheng Feng, Hui Feng and Xin Zhang, "Effect of homogenizing heat treatment on the compressive properties of closed-cell Mg alloy foams". Materials and Design. Vol-49, pp.19-24. (2013).

[35] D.P. Mondal , M.D. Goel, Niharika Bagde, Nidhi Jha, Sonika Sahu, and A.K. Barnwal, "Closed cell ZA27–SiC foam made through stir-casting technique". Materials and Design. Vol-57, pp.315–324, (2014).

Chapter 3

Experimental Work

In the present work, well-known Al-Si alloy LM13 (also known as piston alloy) is used as matrix material, high-purity zircon sand ($ZrSiO_4$) as reinforcement and $CaCO_3$ as blowing agent.

3.1 Materials Used

3.1.1 Matrix Material

In the present work, well-known piston alloy LM13 is used as matrix material. LM13 alloy was obtained in the form of ingots. The compositional analysis of the LM13 alloy was done by wet chemical analysis which is given in Table-4.

Table- 4: Chemical composition of LM13 aluminum alloy.

Element	Si	Fe	Cu	Mn	Mg	Zn	Ni	Al
Chemical Analysis (wt.%)	12.0	0.4	1.2	0.4	1.00	0.2	1.0	Balance

3.1.2 Reinforcement Material

Zircon sand ($ZrSiO_4$) particles were used as a reinforcement material. High purity zircon sand ($ZrSiO_4$) obtained from Indian rare earths Ltd. Mumbai (India) of particle size range (106-25µm) is used as reinforcement. The addition of zircon sand (106-125µm) was done to improve the mechanical properties of the LM13 alloy composite foams.

Table-5: Chemical composition of zircon sand ($ZrSiO_4$).

Elements	ZrO_2 (+HfO_2)	SiO_2	TiO_2	Fe_2O_3
% in Bulk	65.30	32.80	0.27	0.12

Table-6: Properties of zircon sand ($ZrSiO_4$) [4, 5].

Properties	Values
Melting Point ($^{\circ}$C)	2500
Limit of applications (°C)	1850-1880
Hardness (Mohr's Scale)	7.5
Density (g/cm^3)	4.25
Linear coefficient of expansion (10^{-6} K)	4.5
Facture toughness (MPa-m$^{1/2}$)	5
Crystal structure	Tetragonal

3.2 Experimental Procedure

Required quantity of LM13 alloy was taken in a graphite crucible and melted in an electric furnace melt at 750°C. This molten metal was stirred using a graphite impeller at a speed 630 rpm to create the vortex. The impeller blades were designed in such way that it creates vortex. The sand particle was charged inside the vortex at the rate of 20-25 g/min into the melt during stirring with the help of funnel kept on top of vortex. Zircon sand particle of coarse grade (106–125 µm) was selected for present work. Different amount of zircon sand were taken in defined proportion and mixed properly. Subsequently, 2 wt.% $CaCO_3$ powder was charged into the vortex of melt. The stirring was continued for another 5 min even after the completion of particle feeding to ensure homogeneous distribution of the sand particles and allowed the $CaCO_3$ to decompose. Different castings of foam were obtained by following the same route with different holding temperature (800 °C and 850 °C) and holding time 5minuts. After that the crucible is taken out to allow the solidification at room temperature [1].

Table-7: List of processing parameters.

Melting Temperature	750^0C
Total stirring time	10 minutes
Mixing time of blowing agent	3 minutes
Blade angle	45^0
Number of blade	3
Position of stirrer	Up to 2/3 depth in the melt

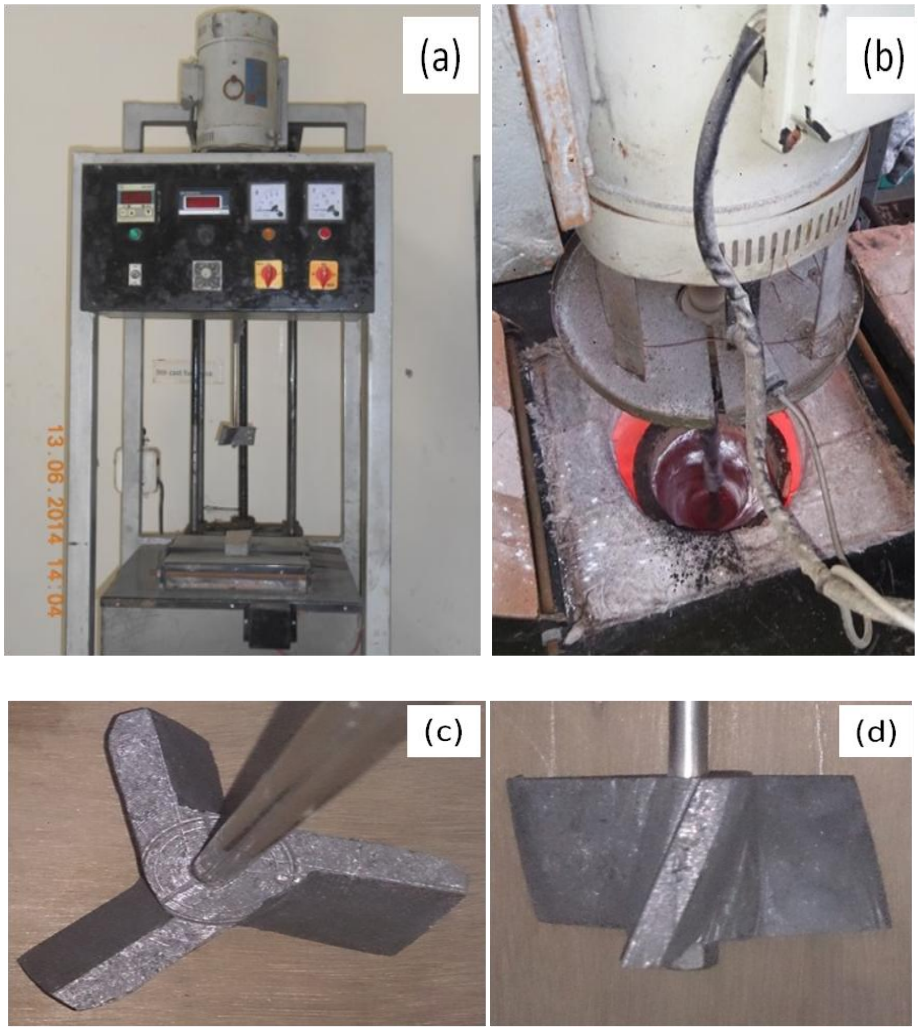

Fig. 3: Stir casting setup: (a) Electric Resistance Furnace, (b) Vertex creation inside the furnace, (c) Graphite impeller used for melt stirring (top view) and (d) Side view.

The method followed for foam preparation is given below in the flow chart:

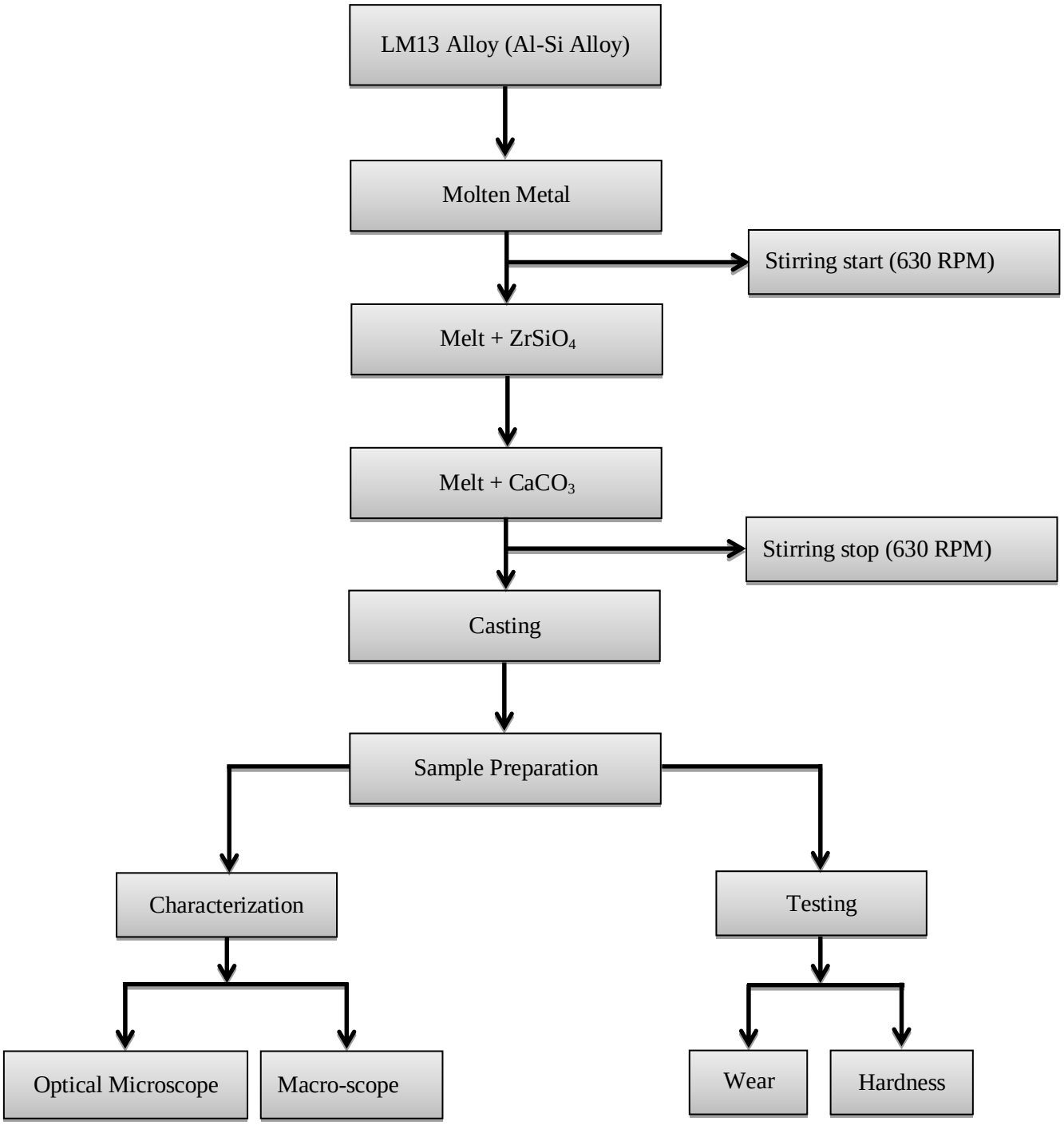

Fig. 4: Methodology of aluminum foam composite [2].

Table-8: Classification of developed aluminum foam sample at different parameter.

Developed Sample / Parameters	$^{0}F_{800}$	$^{0}F_{850}$	$^{2.5}F_{800}$	$^{2.5}F_{850}$	$^{5}F_{800}$	$^{5}F_{850}$
Melting Temperature	750 ºC	750 ºC	750 ºC	750 ºC	750 ºC	750 ºC
Amount of Blowing Agent($CaCO_3$) (wt.%)	2	2	2	2	2	2
Holding Temperature	800 ºC	850 ºC	800 ºC	850 ºC	800 ºC	850 ºC
Amount of Reinforcement (Wt.%)	0	0	2.5	2.5	5	5

3.3 Material Characterization

LM13 alloy foam and LM13 alloy composite foam were characterized using different techniques. Morphological, microhardenss and wear properties of the samples were observed by using optical microscope, macroscope, Vickers hardness and dry sliding wear test using pin-on-disc method.

3.3.1 Optical Microscopy

The foam produced was examined under optical microscope (NIKON, MA-100) to analyze the microstructure. Specimens from different parts of the alloy as well as composite foam of 1x1x3 cm^3 were cut by diamond cutter. These specimens were further ground on 800 up to 1200 grit papers and then polished with 0.5µm diamond polishing paste and etched by Keller's reagent for microstructure analysis. After this, the structure was obtained under optical microscope at different magnifications as shown in Fig 5.

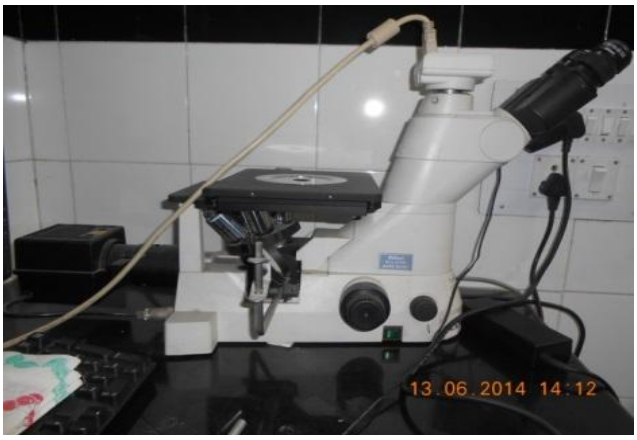

Fig. 5: Image of optical microscope.

3.3.2 Microhardness

The microhardness measured on different phases of the alloy foams and composite foams is given in Table-9. The variation in the size of the indentation reveals that microhardness values significantly depend on microstructural features of the measured area. The composite consists of three different regions: Al matrix, zircon particles, and interface between the Al matrix and zircon sand. Microhardness of the different phases was measured using microhardness tester (Mitutoyo, Japan). Microhardness measurement was done on each set of the observed region (partical, matrix, interface) sample by taking minimum of three indentations per sample at 100 kgf load as shown in Fig 6.

Fig. 6: Image of Vicker's hardness testing machine.

3.3.3 Wear Testing

Dry sliding wear test using pin-on-disc method was done to study of wear behavior of the material. For wear tests a cuboid sample of (1cm × 1cm × 3cm) area was prepared from cast composite foams. The sample was cleaned with acetone to remove dust or grease from the surfaces. Wear tests was performed on wear testing machine (wear and friction monitor, Ducom Instruments, Bangalore, India) as shown in Fig 5 and wear track made of EN32 steel disk having chemical composition (0.14% C,0.52 % Mn,0.18 % Si,0.13 % Ni,0.05 % Cr, 0.06 % Mo,0.019 % P,0.015 % S, balance Fe) and hardness 65 HRC at a relative humidity of 36-56%. The tests were conducted at the loads of 1, 3 and 5kg with the constant sliding velocity of 1.6 ms^{-1}. The wear characteristic has been noted down at room temperature. Before each test the track was cleaned with acetone.

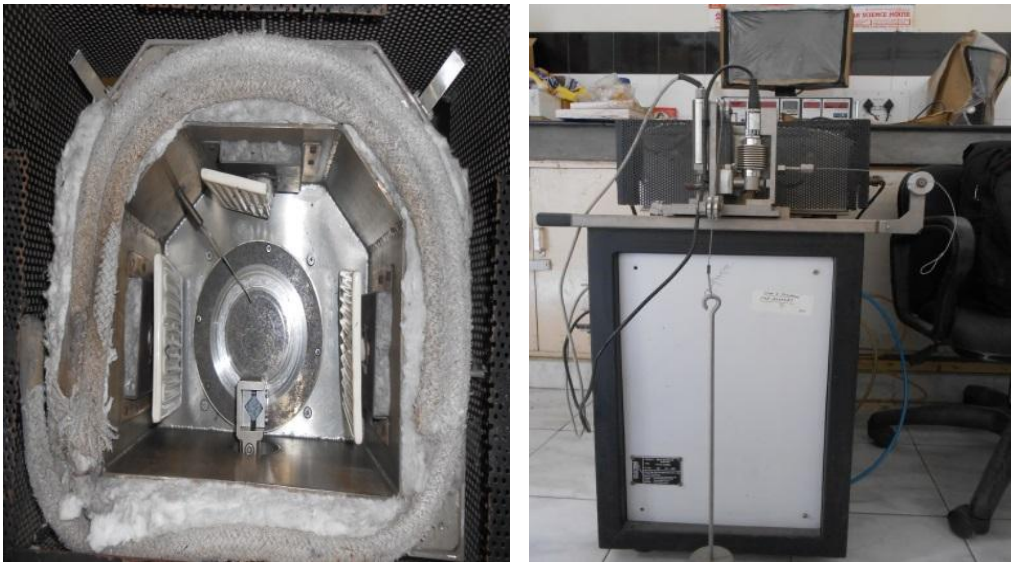

Fig. 7: Image of pin-on-disc wear machine (Ducom-TR-20CH-400).

REFERENCES

[1]. R. Edwin Raj, and B. S. S. Daniel,"Manufacturing challenges in obtaining tailor-made closed-cell structures in metallic foams". Int J Adv Manuf Technol. Vol-38, pp.605-612, (2008).

[2]. Ranvir Singh Panwar, and O.P. Pandey, "Analysis of wear track and debris of stir cast LM13/Zr composite at elevated temperatures". Materials Characterization., Vol-75, pp. 200-213. (2013).

[3] Sanjeev Das, Siddhartha Das, and Karadi Das, "Abrasive wear of zircon sand and alumina reinforced AL-2.5 wt% Cu allot matrix composite-A comparative study". Composite Science and Technology. Vol-67, pp.746-751, (2007).

[4] S.C. Sharma, B.M. Girish, D.R. Somashekar, B.M. Satish, and Rathnakar Kamath, "Sliding wear behavior of zircon particles reinforced ZA-27 alloy composite materials". Wear. Vol-224, pp.89-94, (1999).

Chapter 4

Result and Discussion

The microstructure of LM13 alloy foam and LM13 alloy composite foam with addition of different amount of ceramic reinforcement and their influence on the tribological properties have been studied. Experiments based on different amount of ceramic particles and holding temperature were carried out to investigate the nature of this anomalous behavior. In this work 800 ºC and 850 ºC are the two holding temperatures used in this study. Holding temperature, as an important processing parameter, influences the solubility of gas as well as solidification behavior of LM13 alloy matrix. This implies that holding temperature may have an important impact on cell structure of metal foam. However, little work has been reported on the effect of holding temperature on cell structure of metal foam. In our work, the effect of holding temperature on cell size, porosity, and their distribution are mainly investigated. It can be seen that holding temperature has a great impact on the cell morphology of the LM13 alloy foam. With the increase in holding temperature from 800 ºC to 850 ºC, the cell diameter increases and the distribution of pores observed are homogeneous. Meanwhile, there are few cells which collapse and form irregular spherical cells in the samples at 140 mm from bottom. The density (gm/cm^3) average cell size (mm), average cell wall thickness (µm) and average ligament length (mm) of both LM13 alloy foams ($^{0}F_{800}$ and $^{0}F_{850}$) and LM13 alloy composite foams ($^{2.5}F_{800}$, $^{5}F_{800}$, $^{2.5}F_{850}$, $^{5}F_{850}$) are different, and is shown in Table-9.

Table-9: Effect of the holding temperature on the cell parameters of LM13 alloy foam evolved with 2wt.% blowing agent.

LM13 Alloy Foam	Holding Temperature (°C)	Density (gm/cm^3)	Average Cell Size (mm)	Average Cell Wall Thickness (μm)	Average Ligament Length (mm)
$^{0}F_{800}$	800	0.66	3.4	150	0.40
$^{0}F_{850}$	850	0.63	3.7	125	0.55
$^{2.5}F_{800}$	800	0.72	4.3	230	0.35
$^{2.5}F_{850}$	850	0.69	4.8	350	0.92
$^{5}F_{800}$	800	0.74	3.8	210	1.25
$^{5}F_{850}$	850	0.67	4.2	300	1.85

4.1 Effect of Holding Temperature on Cell Diameter and Their Distribution

4.1.1 LM13 Alloy Foam

The effects of holding temperature on average size of cell in the LM13 alloy foam are shown in Fig 8(a). With increasing holding temperature, the average diameter of cells of the LM13 alloy foam increases. At 800 °C, for sample $^{0}F_{800}$ at a height of 140 mm, the average diameter of cells is 3.4 mm. When holding temperature is increased from 800 °C to 850 °C, the average diameter of cell is 3.7 mm (maximum) at 140 mm from bottom.

Fig 8 shows cell distribution of the LM13 alloy foam fabricated at different holding temperatures ($^{0}F_{800}$ and $^{0}F_{850}$). With increasing holding temperature, the diameter distribution range of cell reduces gradually, which indicates that increasing holding temperature favorably improves the size homogeneity of cell in the LM13 alloy foam. Similarity it is that with increasing holding temperature, the size distribution range of cell increases gradually, which is in good agreement with Fig 8(a).

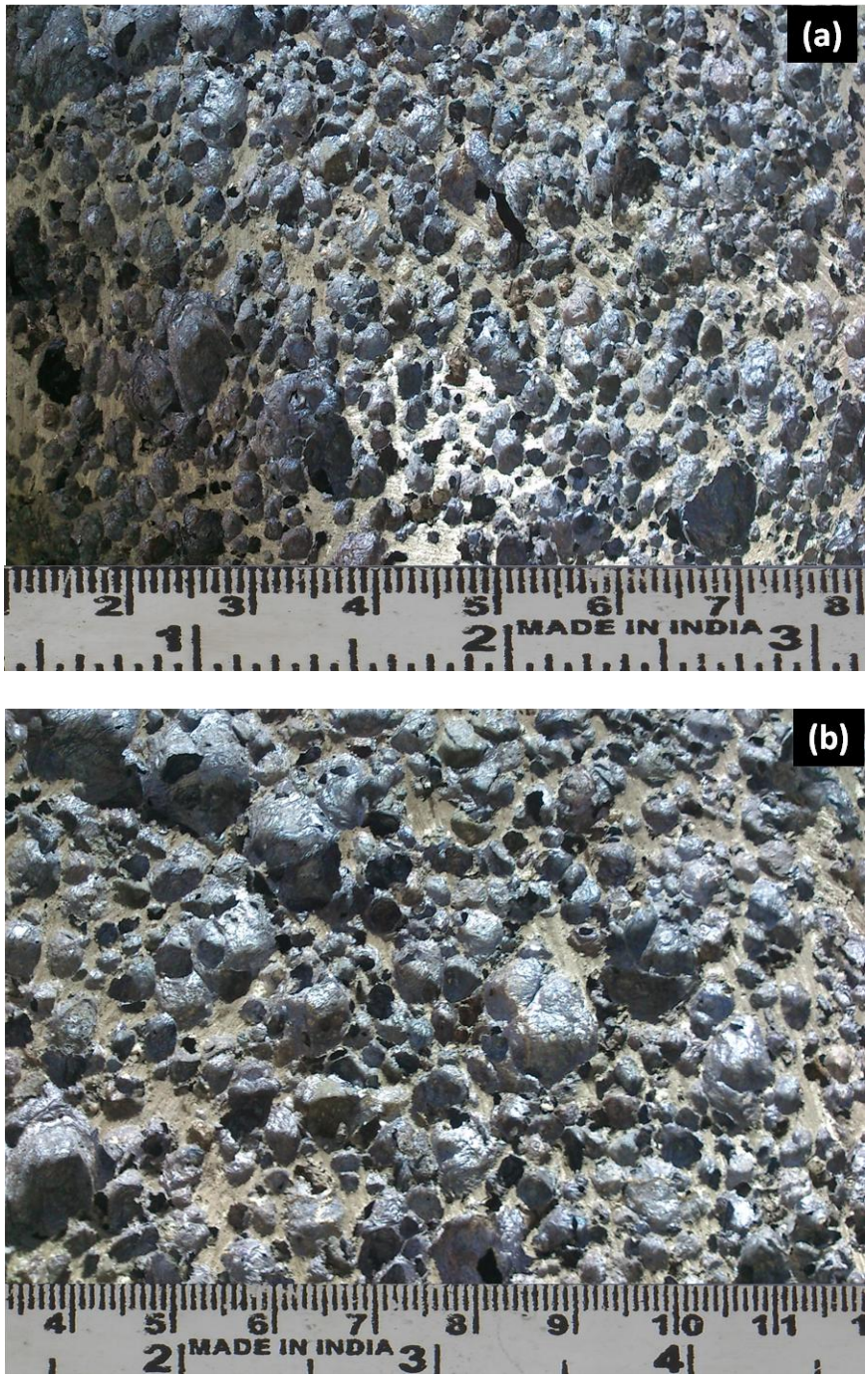

Fig. 8: Macroscopic images of LM13 alloy foam with 2wt.% blowing agent $CaCO_3$ at (a) 800 °C, and (b) 850 °C.

The formation of cell structure is mainly ascribed to cell formation mechanism during preparation of the metal foam. Based on the observation of cell morphology at different holding temperature, three mechanisms are responsible for the process of cell nucleation and growth of the metal foam during unidirectional solidification; nucleation of cell in the solid-liquid

interface, diffusion growth of cell, mergence growth of cell [1]. The size of cell formed by the nucleation of interface between the solid and liquid is small, which is shown in Fig 8(a). The large cell with regular and spherical shape is formed by diffusion growth of small cells, which is shown in Fig 8(a & b). The cells formed by the mechanism of mergence growth of cell result in the formation of large cells with irregular shape, which is shown in Fig 8(b). For the preparation of metal foam at 850 ºC temperature, formation of cell is mainly ascribed to the nucleation of solid-liquid interface and diffusion growth of cell before the disorder stage and the mergence growth of cell dominates over rest of two mechanisms. Therefore, numerous small cells and some large spherical cells tend to merge and form irregular shaped cells. The size distribution of cell is often non-uniform, as shown in Fig 8(b). It can be seen that nucleation rate of the solid-liquid interface increases with holding temperature. This means that with increasing holding temperature, nucleation ability of cells in the solid-liquid interface increases remarkably, and the number of nucleation sites at the solid-liquid interface increases [2]. As a result, the sample fabricated at higher holding temperature ($^{0}F_{850}$) has more cells at 140 mm height. Numerous initial cells with small size are formed due to the large number of nucleation sites at higher holding temperature. Compared with the large cells, the small cells have large capillary pressure, which limits the gas diffusion from liquid phase to the formed cells. In contrast, when holding temperature is low, nucleation rate of cell is low. Meanwhile, the number of cell is small, and the mechanism of diffusion growth of cell is dominated. From Fig 8(a), when the holding temperature is low, the size distribution of cells is inhomogeneous and large spherical cells are formed, which indicates that the growth of cells is mainly ascribed to diffusion controlled mechanism.

4.1.2 LM13 Alloy Composite Foam

Figure 9 shows the microstructure of LM13 alloy composite foam prepared at different holding temperatures (800 ºC and 850 ºC). At 800 ºC, for sample $^{2.5}F_{800}$ at a height of 140 mm, the average diameter of cells is 4.3 mm. When holding temperature is increased from 800 ºC to 850 ºC, the average diameter of cell is 4.8 mm (maximum) for the sample $^{2.5}F_{850}$ at 140 mm from bottom. At 800 ºC, addition of 2.5wt.% ceramic particle in the melt alloy increases the viscosity of the melt. At this condition, nucleation ability of cells in the solid-liquid interface is decreased because the pressure of released gas during decomposition of the $CaCO_3$ is lower as compared to

in base LM13 alloy. This gas expands in the liquid metal and creates bubble like structure on the surface of the melt, forming liquid foam which is stabilized by the presence of solid ceramic particles on the gas liquid interfaces of the cell walls [3, 4]. The variable amount of the addition of the zircon particles was done so as to study its effect systematically on the cell structure. In the stabilization of the LM13 alloy composite foam, the wettability of the zircon sand particles is not the only dominant property but foam stability is also greatly dependent on the drainage and rupture of the cell wall separating the air bubbles. Foam stability may increase or decrease, depending on the role of the zircon sand particles on the drainage and rupture process [5]. The presence of zircon sand particles in the composite melt increases the liquid viscosity, and the higher viscosity slows down liquid flow and thus retards the cell wall drainage before it solidifies. Apart from their influence on melt viscosity, the zircon sand particles have an important impact on composite foam stability through their attachment to the gas/liquid interface of LM13 alloy foam.

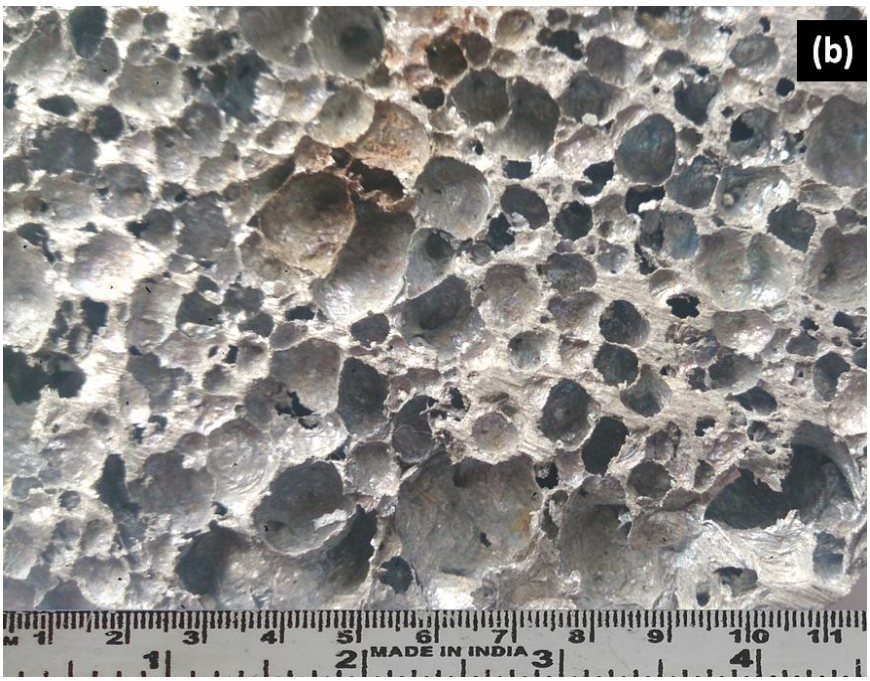

Fig. 9: Macroscopic images of LM13 alloy composite foam with 2wt.% blowing agent $CaCO_3$ and 2.5wt.% $ZrSiO_4$ at (a) 800 ℃, and (b) 850 ℃.

This further changes the interfacial curvatures and reduces the capillary pressure difference between the ligament length and the cell wall of the LM13 alloy composite foam. Because most of the particles are segregated at the liquid/gas interface of LM13 alloy composite foam [6]. The concentration range from 2.5wt.% to 5wt.% of the particles is critical for stable holding of the composite slurry. However, the actual concentration required to form stable foam depends largely on the immersion depth of the gas exit, because the number of particles encountered and picked up by the gas bubbles is dependent on the distance traveled by the bubbles [6]. Furthermore, the rising bubbles become stable only when the critical surface coverage by zircon sand particles is achieved. Therefore, a lower critical concentration is required to produce the longer travelled path of bubble for a stable foam.

The cell size of the LM13 alloy composite foam is decreased with decreasing pressure of released gas in the melt which is shown in Fig 9(a). At 800 ºC, 2wt.% blowing agent with 2.5wt.% zircon sand particles ($^{2.5}F_{800}$) did not produce sufficient pressure for making uniform cell size composite foam Fig 9(a). It is worth noting that the increment in the holding temperature (from 800 ºC to 850 ºC) leads to increase in the diameter of cell size of the LM13 alloy composite foam ($^{2.5}F_{850}$) as the viscosity of melt decreased which is shown in Fig 9(b). Two

neighboring bubbles in the melt are separated by a liquid film in the liquid foam. The liquid film tends to flow due to surface tension [7]. Evidently, the node size and ligament length of both are increased with the increase in cell size [8]. The results indicate that the gas flow rate changes the cell size because of the addition of ceramic particles.

The increment in amount of reinforced particle from 2.5wt.% to 5wt.% with different holding temperature (800 ºC and 850 ºC) was also done. At 800 ºC, for sample $^{5}F_{800}$ at a height of 140 mm, the average diameter of cells is 3.8 mm, which is shown in Fig 10(a). When holding temperature is increased from 800 ºC to 850 ºC, the average diameter of cell is 4.2 mm (maximum) for sample $^{5}F_{850}$ at 140 mm from bottom, which is shown in Fig 10(b). It is worth noting that the increments in the amount of zircon sand from $^{2.5}F_{800}$ to $^{5}F_{800}$ lead to increase in the viscosity of melt that leads to decrease in cell size. But, the increment in the holding temperature from $^{5}F_{800}$ to $^{5}F_{850}$ leads to decrease in the viscosity of melt and cell size increased, which is shown in Fig 10. Zircon particles may occupy the area on walls of cell and also at triple point (node). Since some particles can be easily dragged by upcoming gas so they may occupy the cell wall area and some particles may move towards the corner. It is interesting to note that fluid follows the contour and as per Coanda effect [9], this type of distribution is possible. This may lead to the variation in cell size, node size and ligament length of the LM13 alloy composite foams. In the presence of the $ZrSiO_4$ particles, the produced liquid foam becomes stable. So the structure can be easily manipulated. In sample $^{5}F_{850,}$ the rate of decomposition of $CaCO_3$ becomes higher, so the equilibrium carbon dioxide gas pressure also increases. Due to the decrement in the viscosity of the melt alloy and increment in the decomposition rate of blowing agent, the cell formation becomes easier [1, 6]. This is responsible to generate uniform cell size for stable holding of the composite slurry Fig 10(b). The wettability of the ceramic particles by the alloy melt is not the only dominating factor but also to provide the stability for the foam which is greatly dependent on the drainage and rupture of the cell wall separating the gas bubbles. The role of the particles on the drainage and rupture process affects the foam stability. The effect of melt viscosity in terms of the interfacial curvatures and the cell wall of the aluminum composite foam can be observed from the microstructures of the produced foams. The cell size and cell wall thickness of the $ZrSiO_4$ based foams is significantly changed, which is shown in Fig 10.

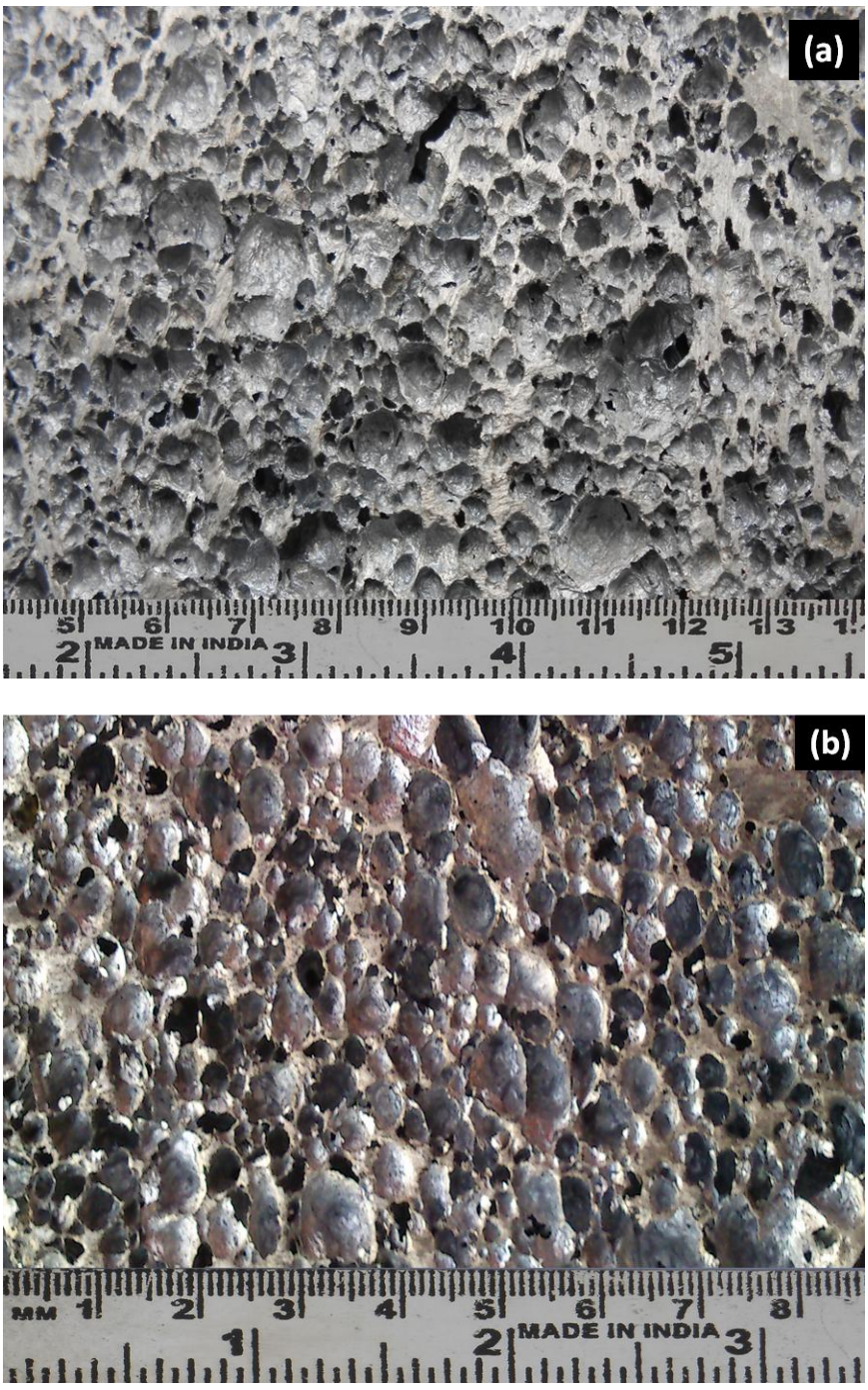

Fig. 10: Macroscopic images of LM13alloy composite foam with 2wt.% blowing agent $CaCO_3$ and 5wt.% $ZrSiO_4$ at (a) 800 °C, and (b) 850 °C.

4.1.3 Effect of Holding Temperature on Cell Morphology of LM13 Alloy Foam and LM13 Alloy Composite Foam

The cell size of the LM13 alloy composite foam got increased with increasing rate of released CO_2 which depends on the decomposition rate of $CaCO_3$. At holding temperature of 800 ºC, the 2wt.% $CaCO_3$ used as blowing agent results in smaller size of cell wall thickness in comparison to the larger size of cell wall thickness produced at 850 ºC holding temperature as can be seen in Fig 11(a-b).

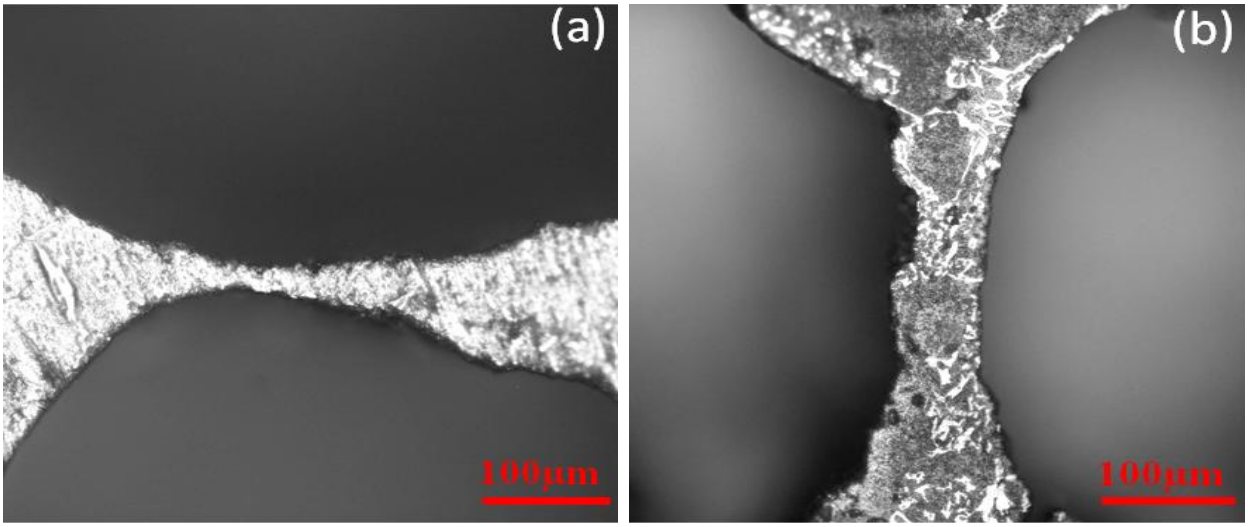

Fig. 11: Optical image of 2wt.% $CaCO_3$ showing variation in cell wall thickness and node size of the LM13 alloy foams processed at (a) 800 ℃, and (b) 850 ℃.

The thickness of the cell wall increases with increasing zircon sand concentration, as shown in Fig 12(a-b). The increase in the thickness of the cell wall at certain particle size implies that the viscosity of the composite melt is becoming higher and higher as more particles are incorporated into the liquid aluminum. Moreover, the increase in cell wall thickness also means that more aggregation of particles in the particle/liquid interface creates a more tortuous path for the liquid and acts as a liquid flow barrier from the cell wall towards the plateau border resulting the cell wall drainage [4, 10]. The retardation in cell wall drainage, results the increment in cell wall thickness. Therefore, it can be said that the increase in holding temperature from 800 ºC to 850 ºC during the preparation of the LM13 alloy composite foams has a great effect on the cell size.

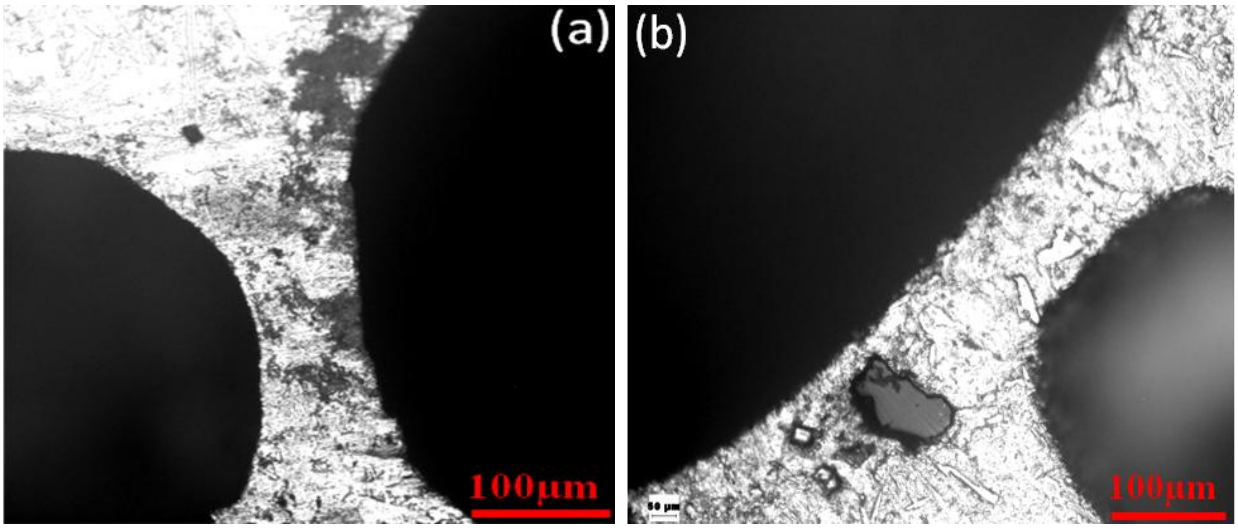

Fig. 12: Optical images of 2wt.% $CaCO_3$ showing variation in cell wall thickness and node size of the LM13 alloy composite foams with different amount of reinforcement at 800 ℃ (a) 2.5wt.%, and (b) 5wt.%.

Figure 13(a-b) shows the cell wall thickness and node size of the LM13 alloy composite foams prepared with different contents of zircon sand reinforcement. At 850 ºC holding temperature, the node size of the cell is smaller with thinner ligament Fig 13(a). The foam cell does not coalesce to form a bigger bubble even it comes into contact with other cells during its floatation to the surface of the melt due to lower viscosity. When increased the amount of zircon sand from 2.5wt.% to 5wt.% at 850℃, the node size of the cell is larger with thick ligament due to the increase viscosity of melt alloy as shown in Fig 13(b). Thus, the enlargement of the cell size is not caused by higher gas release rate but due to increase in the frequency of bubble collision due to more turbulent flow of the melt and more generation of the cells, but contributed by the higher probability of particle attachment to the rising bubbles at higher gas flow rate [11]. The mechanical properties of foams are largely determined by their density and microstructure. In addition, the cell uniformity as well as cell size, node and structure are also important factors determining the properties of foam. The characteristics of cell may be quite different in metal foams produced by different routes, thus resulting in different mechanical properties [12]. Therefore, it is not suitable to compare the data of mechanical properties for foams obtained by different processes, even for the same cell wall material. The mechanical properties of foam materials are related not only to the properties of cell wall material but also the cell geometry.

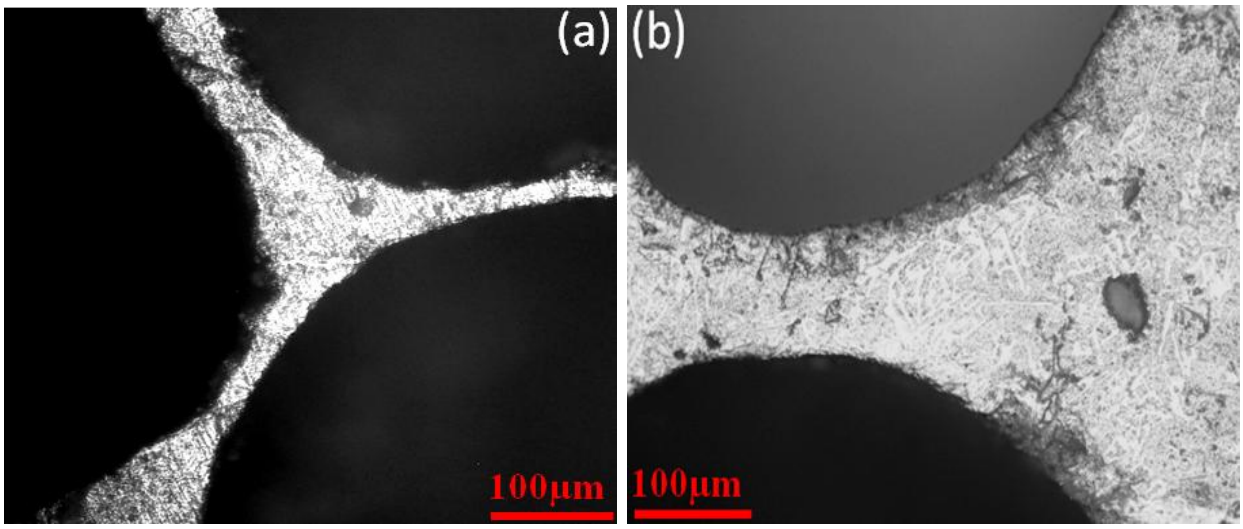

Fig. 13: Optical images of 2wt.% $CaCO_3$ showing variation in cell wall thickness and node size of the LM13 alloy composite foams with different amount of reinforcement at 850°C (a) 2.5wt.%, and (b) 5wt.%.

The experimental results show that the increase in holding temperature with addition of ceramic particles in LM13 alloy composite foams decreases the cell wall thickness. These experimental results indicate that holding temperature and decomposition rate of blowing agent is responsible to change the morphology and structure of the closed cell composite foams which is shown in Fig (12 and 13).

The experiments clearly show that zircon particles within the metallic melt are a prerequisite for a stable foam. Explanations given for this finding often address the influence of such particles on bulk viscosity of melts [5, 6]. As viscosity is increased by dispersion of particles, this would slow down the extraction of melt from the films by gravitational and capillary forces. In thin films the effect of particles could be even more important due to surface effects and a hypothetical particles build-up near the thinnest section causing a jamming of liquid.

The pure LM13 alloy foams show a thick layer of Al melt at the bottom of the foams after the maximum expansion achieved, indicating continuous drainage of liquid through the foam structure. Moreover, the extensive drainage removed the liquid from ligament length and cell walls, resulting in the rupture of pores when the thickness of the cell wall was less than the critical cell wall thickness [12]. The effect of heavy drainage can also be seen from the non-uniform foam structure with irregular cell size and shape of the LM13 alloy foams. The addition of zircon sand in the LM13 melt alloy, the cell structure of the composite foams was more

uniform. At 850 ºC, the LM13 alloy composite foams have higher circular cell than the LM13 alloy foams at 800 ºC, as shown in Fig (12 and 13), indicating more uniform cell structure of the foams. The improvement of LM13 alloy composite foams structure is thought to result from increasing bulk liquid viscosity and decreasing surface tension. Due to the presence of zircon particles in ligament length and cell walls, reduction in the rate of drainage and cell coalescence occurs. As the surface tension decreases, cells are allowed to expand further with spherical morphology, minimizing the surface energy of the system. Fig 13(b) presents the cell wall surface of LM13 alloy composite foams with 5 wt.% zircon sand ($^{5}F_{850}$). It is clear that the addition of zircon particles changes both morphology and characteristics of the cell wall surface. Most particles were embedded into the cell wall surface, protruding only some parts of the particles, indicating the good wetting of the particles. Figure 13 shows the presence of zircon particles in a ligament length and cell wall. The wetting of the zircon particles, through the chemical reaction, is likely to strengthen the cell walls and enable them to thin down to a greater degree prior to rupture.

4.2 Microhardness Analysis

Microhardness measurement on the alloy matrix of LM13 alloy foam has been taken. The effect of reinforced particulates on LM13 alloy composite foam at different phases of composite has been taken. Reinforced particles show high hardness which decreases as we move away from particle in the composite foam.

Table-10: Variation of microhardness of LM13 alloy foam and LM13 alloy composite foam different phases of composite foam.

Microhardness (Hv)				
Composite Foam	**At Particle**	**At Matrix**	**At Interface**	**At Node**
$^{0}F_{800}$	-	69.49± 0.30	-	69.60± 0.25
$^{0}F_{850}$	-	68.28± 0.25	-	70.54± 0.25
$^{2.5}F_{800}$	643.45± 0.15	78.54± 0.25	118.72± 0.30	78.91± 0.25
$^{2.5}F_{850}$	635.93± 0.15	80.88± 0.25	126.19± 0.30	78.10± 0.25
$^{5}F_{800}$	667.22± 0.20	85.60± 0.25	130.92± 0.30	86.40± 0.25
$^{5}F_{850}$	651.24± 0.20	82.77± 0.30	128.65± 0.30	84.30± 0.25

The high hardness at particle/matrix interface indicates good interfacial bonding between particle and alloy matrix. This phase at particle/matrix interface exhibits higher hardness in comparison to the matrix phase and also binds the particles with matrix. Composite containing 5 wt.% zircon sand ($^5F_{850}$) shows high microhardness value at particle, interface, and matrix which is achieved by good interfacial bonding and refinement of microstructure. The indenter marks as a square base pyramid shaped diamond is present on the sample foam. The indenter marks size is increased as we move away from matrix to particles which seen in Fig 14(a and b).

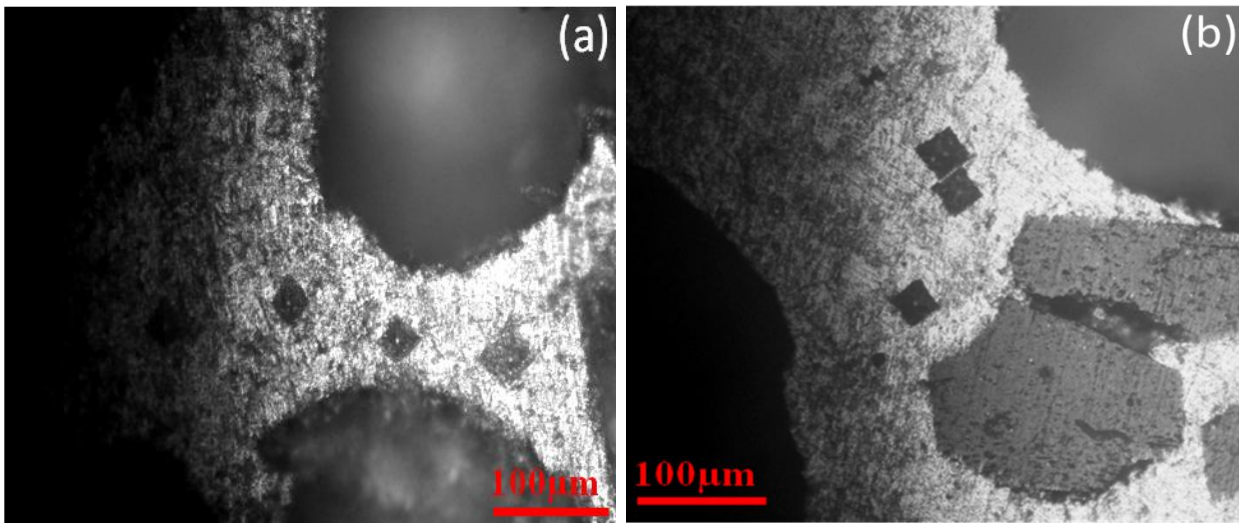

Fig. 14: Optical images of 2wt. % $CaCO_3$ showing variation in cell wall thickness and node size of (a) the LM13 alloy foams and (b) composite foam with 5wt.% amount of reinforcement at 850 ℃.

4.2.1 Wear Analysis of LM13 Alloy Foams and LM13 Alloy Composite Foams at Different Loads

Progressive loss of material from the operating surfaces as a result of relative motion is known as wear. In order to get idea about the durability of the materials under different conditions (like load and temperatures), the prepared samples were tested under dry sliding wear conditions. Figure 15 represents the variation of the wear rate as a function of sliding distance for LM13 alloy foam under dry condition at different loads. Effect of applied load on wear behavior of LM13 alloy foam and LM13 alloy composite foam was studied at 1, 3, and 5 kg loads.

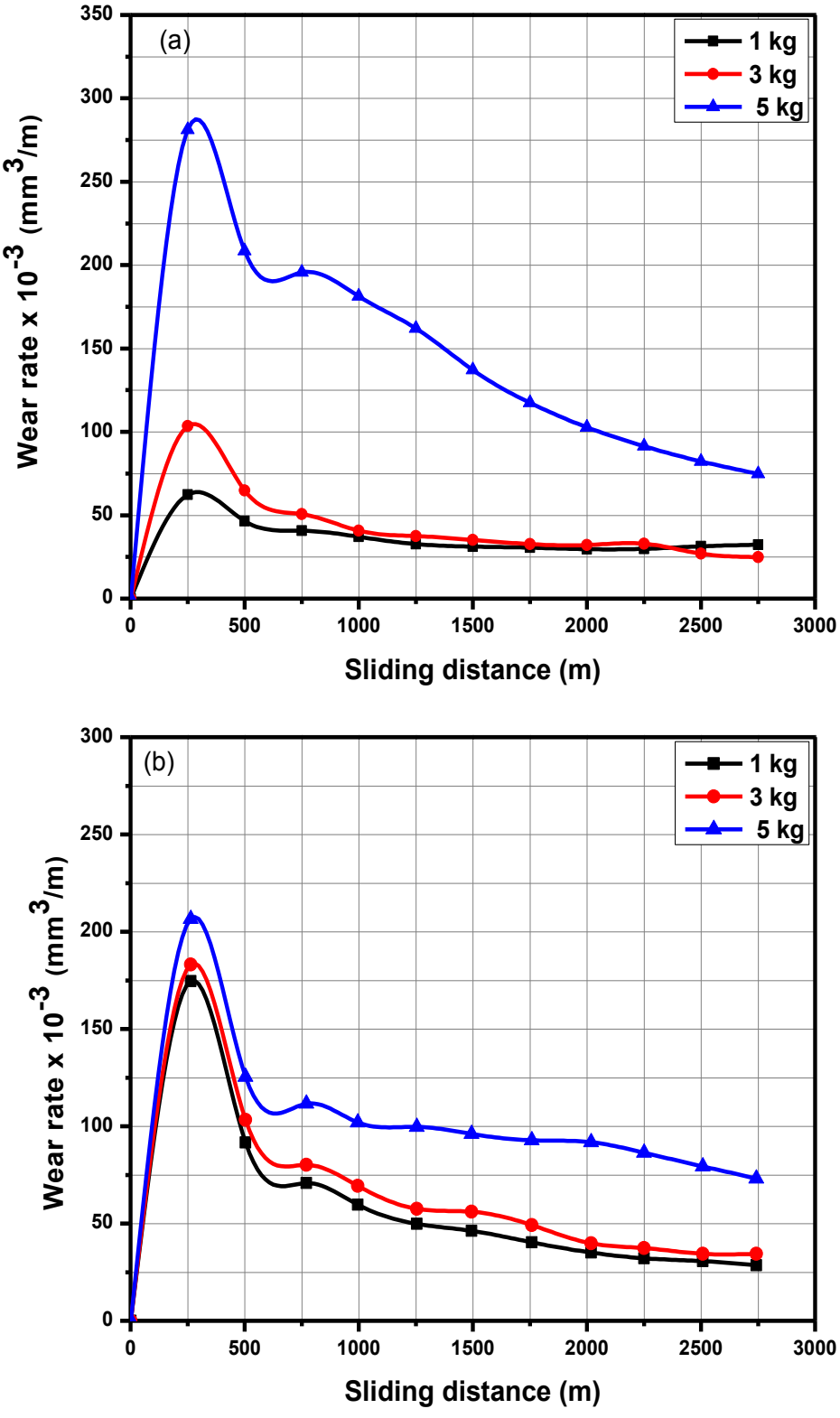

Fig. 15: Wear rate against sliding distance of LM13 alloy foam 2wt.% blowing agent $CaCO_3$ at (a) 800 ℃, and (b) 850 ℃.

Wear rate vs. sliding distance graphs of the LM13 alloy foam, measured at room temperature are shown in Fig 15(a). It is evident from the figure that there is a rise in wear rate at the initial stage. This may occur due to a sudden shear force is applied on the cross-sectional area of specimen by the steel disc at the initial stage of wear [1]. Once initial transition period (run in wear) comes to an end the wear rate of the LM13 alloy foam drops and a steady state value of wear rate is attained. However, with the increase in applied load from 1 to 3 kg, wear rate of LM13 alloy foam is increased. There is a sharp change in wear rate at high load (5 kg) with respect to low load (1 and 3 kg). During wear when two contact surfaces slide against each other, there will be some squeezing out phenomenon of the adsorbed films. When the applied load is increased from 1 to 5 kg, contact pressure on the ligament and node becomes higher, the cell may fracture and some plateau material slide over the cell. After some sliding, there will be a layer of turbulently mixed substances, some of which will fall out as wear debris, but most of which will remain as a transfer film. The contact area between counter surface and foam sample surface depends on the cell size of the LM13 alloy foam. The contact area is increased due to decrease in the cell size of the LM13 alloy foam and wear rate is decreased. Therefore, the load transfer phenomenon depends on the contact area and the deformation rate of the cell wall of the foam sample is decreased, which is responsible to decrease the wear rate of the LM13 alloy foam. The cell size of $^{0}F_{850}$ is larger as compared to $^{0}F_{800}$. The increased size of ligament at 850 ºC results the decreased contact interface area between foam sample and steel disc surface. Under such conditions, contact surface has not enough adhesive bonding strength to resist relative sliding which leads to a small plastic deformation caused by dislocation movement which is introduced in the contact region under compression and shear loading conditions. Wear rate of sample $^{0}F_{850}$ is higher as compared to sample $^{0}F_{800,}$ which is shown in Fig 15(a and b). The actual contact area generally depends on the cell size of composite foam sample. Initially the wear rate is higher which corresponds to the run in wear. However, the steady states wear approaches at nearly 1500 m sliding distance. Run-in wear of LM13 alloy composite foam is higher at 5 kg load as compared to at 1 kg loads as shown in Fig 16. The wear behavior of the composite sample $^{5}F_{800}$ at different loads against sliding distance is shown in Fig 17(a). It shows that at steady state wear is approachable after a sliding distance of 1000 meters. At 1kg, and 3 kg loads, the wear rate correspondingly decreases with sliding distance and approaches the steady state after 1500 meters of sliding distance. Steady state wear is approached after 2000 meters in case of 5kg load.

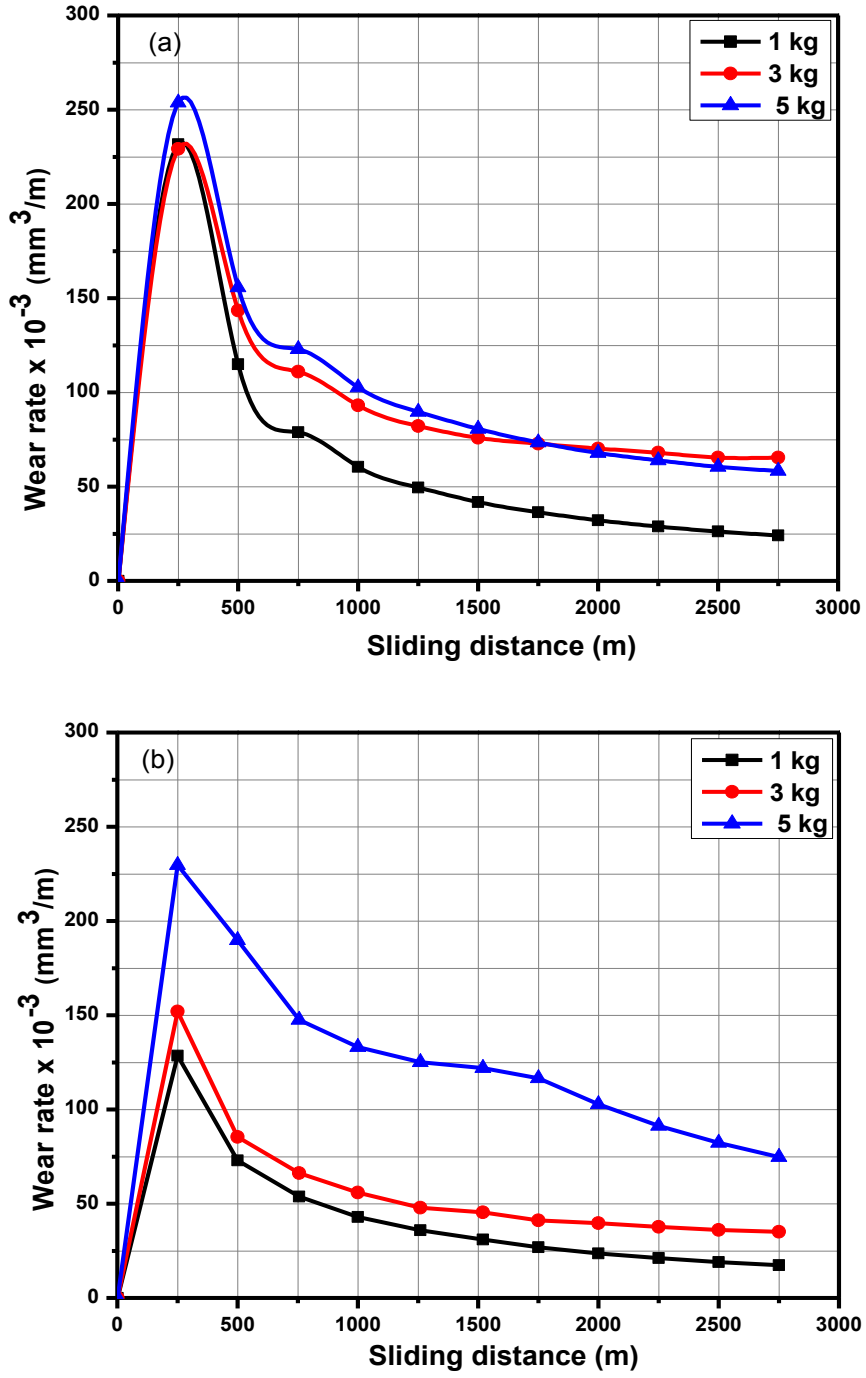

Fig. 16: Wear rate against sliding distance of LM13 alloy composite foam 2wt.% blowing agent $CaCO_3$ and 2.5wt.% $ZrSiO_4$ at (a) 800 ℃, and (b) 850 ℃.

In the case of $^{2.5}F_{800}$ and $^{2.5}F_{850,}$ it is observed in Fig.16 (a and b) that wear behavior of the LM13 alloy composite foam is similar at room temperature for all loads. However, the wear rate of

LM13 alloy composite foam increases with the increase in applied load. The increase in wear rate may be due to the increase in the actual contact area between composite sample and disc. Wear behavior of composite sample $^{5}F_{850}$, the run-in wear is higher as compared to composite sample $^{5}F_{800}$ at all loads. The steady state wear is approachable after the sliding distance of 2000 meters for 1kg and 3kg load. The difference in wear rate of 1kg, 3kg and also in 5kg is relatively small. At 5kg load steady state wear is reached at 1500 meters of sliding distance. The cell size of the LM13 alloy composite foam ($^{2.5}F_{800}$, $^{5}F_{800}$) is smaller as compared ($^{2.5}F_{850}$, $^{5}F_{850}$) which is shown in Fig (16 and 17). LM13 alloy composite foam ($^{2.5}F_{800}$, $^{5}F_{800}$) exhibits better wear resistance as compared to LM13 alloy composite foam ($^{2.5}F_{850}$, $^{5}F_{850}$). The results for the composites presented in Fig 16(a) and 17(b) also show the initial stage variation which indicate the grinding of asperities on the contact surface of the sample as indicated by the high wear rate with respect to increased loads.

It is observed that wear rate of LM13 alloy composite foam ($^{2.5}F_{800}$, $^{5}F_{800}$) decreases sharply as compared to LM13 alloy composite foam ($^{2.5}F_{850}$, $^{5}F_{850}$) at all loads. Moreover, the edges of zircon sand are sharp which further assist to cut the counter face disc on which the specimen is rotating. During this action, the sharp edges of the abrading zircon sand particles become blunt. This helps in decreasing the wear rate. The shape of the zircon sand particles also plays an important role to decrease wear volume of the LM13 alloy composite foam. At the higher load, frictional heat generated between composite foam sample and steel disc is responsible to soften the cell wall. When the high load is applied on the less contact area, these soften cell wall gets plastically deformed and deformed material flow over the cell [13]. After some time, this deformed material is cooled and works as increased contact area which supported to decrease wear rate of the foam material. Addition of zircon sand reinforcement in the matrix alloy leads to considerable variation in tribological behavior of the alloy. The tribological properties may vary with the variation of zircon sand content in the matrix alloy, and thus there is a need to examine the effect of zircon sand content on the sliding wear behavior of the LM13 alloy composites foam. Fig 16(a) represents the wear rate as a function of zircon sand content at different applied load. It is evident from these Figs (16 and 17) that the wear rate decreases linearly with increasing zircon sand content and increases with increasing applied load. It is also depicted that the wear rate of LM13 alloy composites foam ($^{2.5}F_{800}$, $^{5}F_{800}$) at 5kg load is considerably less as compared of LM13 alloy composites foam ($^{2.5}F_{850}$, $^{5}F_{850}$).

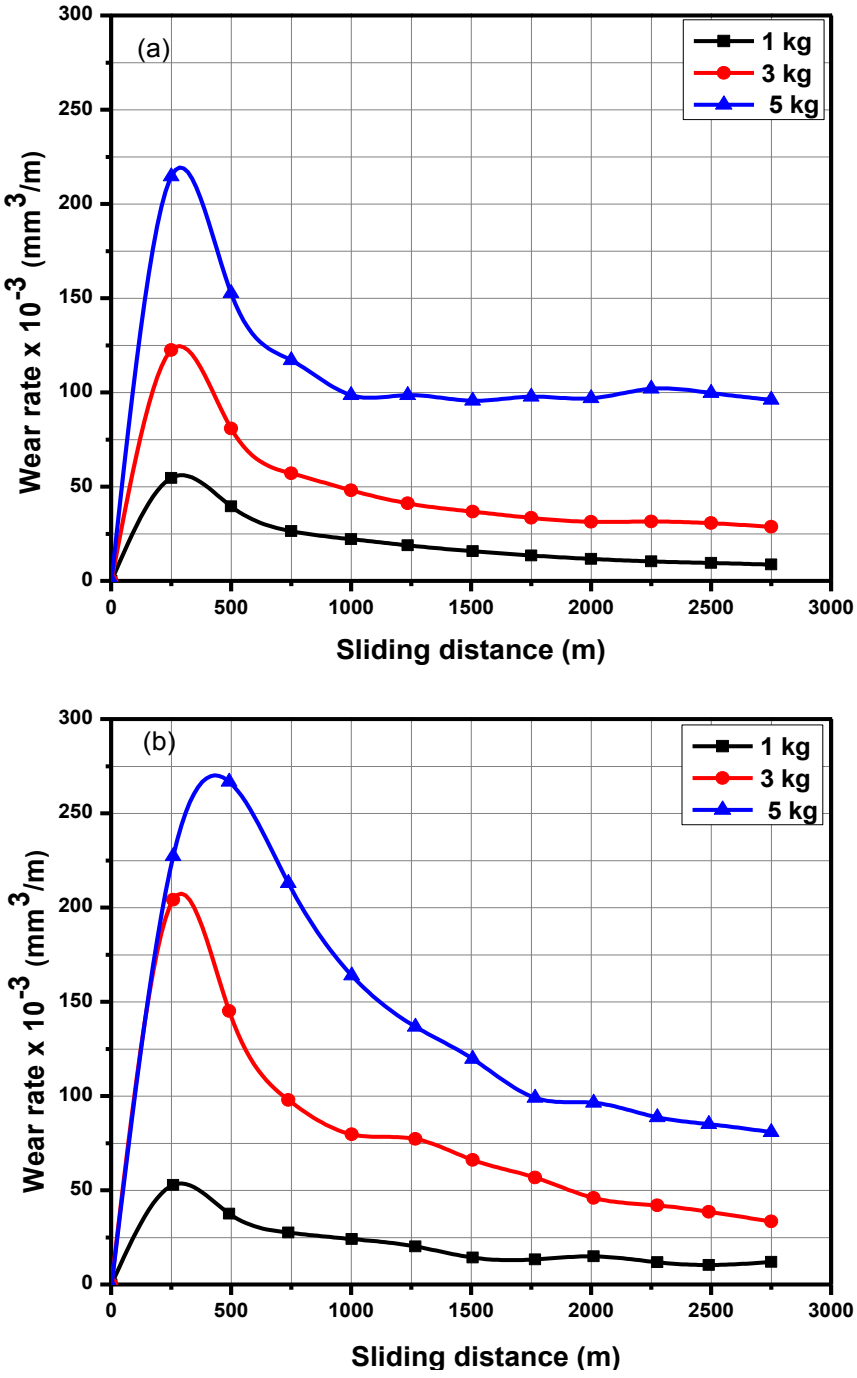

Fig. 17: Wear rate against sliding distance of LM13 alloy composite foam 2wt.% blowing agent $CaCO_3$ and 5wt.% $ZrSiO_4$ at (a) 800 °C, and (b) 850 °C.

When the content of zircon sand is increased form 2.5wt.% ($^{2.5}F_{800}$) to 5wt.% ($^{5}F_{800}$) in the of LM13 alloy composites foam at 800 ºC, cell size of the foam is decreased due to the increase in the viscosity of melt alloy at this temperature. As the zircon sand content increases, the degree of effective contact between the asperities of composite foam surface and counter surface decreases

and thus, the wear rate of composite reduces with increase in zircon sand content. The higher content of zircon sand in matrix alloy is responsible for restricted heat flow, which is generated by frictional motion. In this case, the cell wall is not easily plastically deformed because the frictional heat is not sufficient to soften the cell wall of composite foam sample. The larger cell size exhibit higher wear rate of the sample ($^{2.5}F_{800}$, $^{5}F_{800}$) as compared to small cell size composite foam sample ($^{2.5}F_{850}$, $^{5}F_{850}$), which is shown in Fig (16 and 17). The large cell size of the composite foam has less contact area between composite foam and steel disc during the rotational motion condition. At this condition, frictional heat generates on the contact area is sufficient for plastic deformation of cell wall in the sliding direction and wear rate of the composite foam is increased.

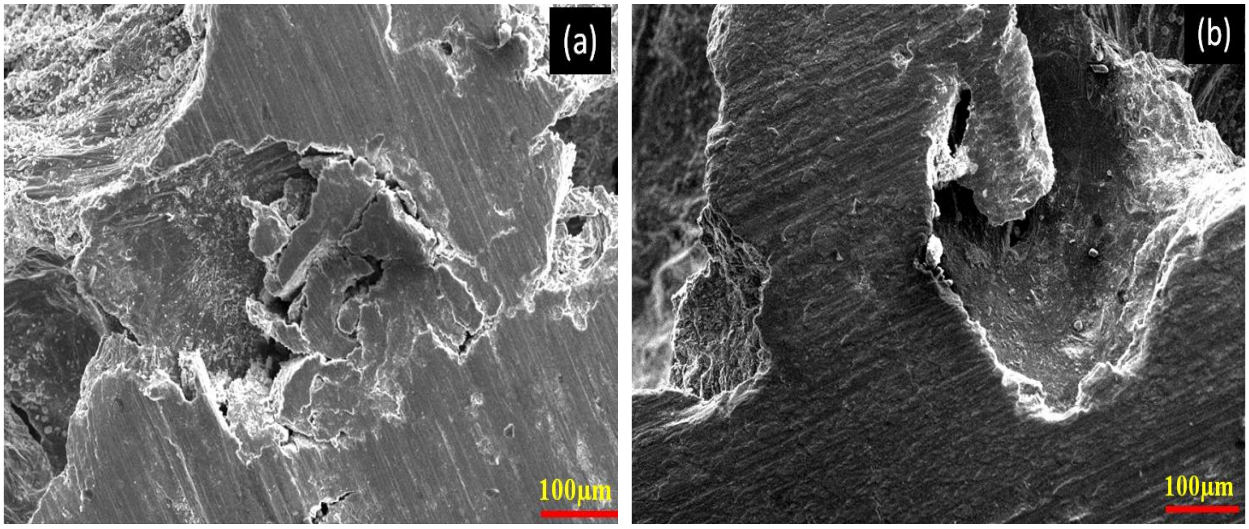

Fig. 18: The SEM micrograph of worn pin surface of foam sample $^{0}F_{800}$ at (a) 1kg and (b) 5kg.

The worn surface of foam sample $^{0}F_{800}$ when tested at different loads of 1 kg and 3 kg and sliding velocity of 1.6 ms^{-1} is shown in Fig 18. It depicts continuous wear grooves and craters and some cell plastically deformed under applied load Fig 18(a). The same sample when tested at 5 kg load, the wear surface is characterized with continuous and deeper wear grooves along with craters, which are relatively more elongated Fig 18(b). This figure also shows greater extent of wear debris accumulation in the craters, which make the surface relatively rough. The surface also demonstrates the formation of mechanical mixed layer (MML) to a greater extent.

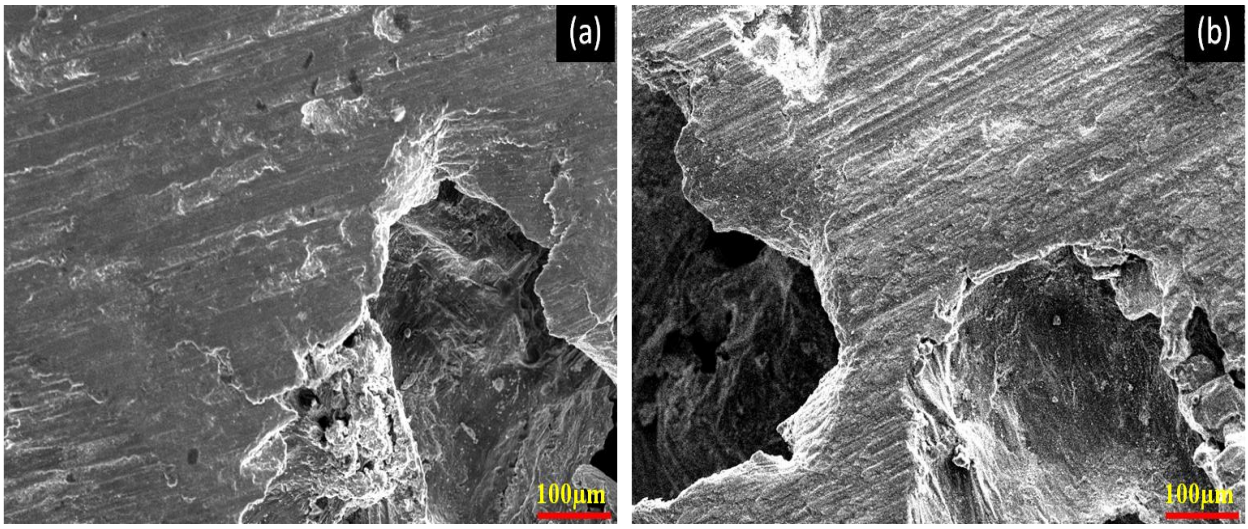

Fig. 19: The SEM micrograph of worn pin surface of composite foam sample $^{5}F_{800}$ at (a) 1kg and (b) 5kg.

Figure 19 (a and b) shows that wear track of composite foam sample $^{5}F_{800}$. In Fig 8(a), grooves were formed in the soft metal cells and there was a small amount of the metal that became smeared around the cell edge and over the ceramic struts. More metal became smeared and a larger area of the worn scar was covered by the smeared metal. When the applied load is increased from 1kg to 5kg, the worn surface of the composite foam sample $^{5}F_{800}$ is more as observed from the Fig 19(b). Delamination wear is the main cause of the loss of material. However, at 5kg load some intact portion of the composite sample $^{5}F_{800}$ is observed with grooves caused by the abrasion. From rest of the portion the material has chipped out because of the crack initiation near the cell wall and in the vicinity of the reinforced particle due to generated high stress. The wear loss is in the form of chips coming out from the material and oxidative layer no longer have the capability to withstand high stress due to load and thermal softening [14].

REFERENCES

[1] J. Daniel Bryant, Deborah Wilhelmy, Jacob Kallivayalil and Wei Wang, "Development of aluminum foam processes and products". Materials Science Forum. Vol-521, pp.1193-1200, (2006).

[2] Marco Haesche, Dirk Lehmhus, Jorg Weise, Manfred Wichmann and Irene Cristina Magnabosco Mocellin, "Carbonates as foaming agent in chip-based aluminum foam precursor". Journal of Material Science and Technology. Vol-26, pp.845-850, (2010).

[3] M. Mukherjee, F. Garcia-Moreno and J. Banhart, "Solidification of metal foams". Acta Materialia. Vol-58, pp.6358-6370, (2010).

[4] Alexandra Byakova, Svyatoslav Gnyloskurenko and Takashi Nakamura, "The role of foaming agent and processing route in the mechanical performance of fabricated aluminum foams". Metals. Vol-2, pp.95-112, (2012).

[5] M. Malekjafarian and S.K. Sadrnezhaad, "Closed-cell Al alloy composite foams: Production and characterization". Materials and Design. Vol-42, pp.8-12, (2012).

[6] Alexander Dudka, Francisco Garcia-Moreno, Nelia Wanderka and John Banhart, "Structure and distribution of oxides in aluminum foam". Acta Materialia. Vol-56, pp.3990-4001, (2008).

[7] M.F. Ashby, A.G. Evans, N.A. Fleck, L.J. Gibson, J.W. Hutchinson and H.N.G. Wadley, "Metal Foams: A design guide". Butterworth-Heinemann. (2000).

[8] Sheng-Chung Tzeng and Wei-Ping Ma, "A novel approach to the manufacturing and experimental investigation of closed-cell Al foams". The International Journal of Advanced Manufacturing Technology. Vol-32, pp.473-479, (2007).

[9] Imants Reba, Scientific American Inc. 84, 214 (1966).

[10] Takuya Koizumi, Kota Kido, Kazuhiko Kita, Koichi Mikado, Svyatoslav Gnyloskurenko, and Takashi Nakamura, "Method of preventing shrinkage of aluminum foam using carbonates". Metals. Vol-2, pp.1-9, (2012).

[11] Paul H. Kamm, F. Garcia-Moreno, Catalina Jimenez and J. Banhart, "Suitability of various complex hydrides for foaming aluminum alloys". Journal of Materials Research. Vol-8, pp.2044-5326, (2013).

[12] Louis-Philippe Lefebvre, John Banhart and David C. Dunand, "Porous metals and metallic foams: Current status and recent developments". Advanced Engineering Materials. Vol-10, pp.775-787, (2008).

[13] B. kriszt, U. Martin and U. Mosler, “Characterization of cellular and foamed metals, ch.4.1, in Handbook of cellular metals”. (Ed.:H.P.Degischer and B.Kriszt), WILEY VCH, Weinheim, pp.130-145, (2002).

[14] L.J. Gibson and M.F. Ashby, “Cellular solids: structure and properties”. (1997).

Chapter 5

Conclusions and Future Works

5.1 Conclusion

The production of LM13 alloy foam requires a good control of the parameters which affect the stability of the formed bubbles in the melt alloy. The most favorable condition to achieve stability of the bubbles were: holding temperature close or below the liquidus temperature of the LM13 alloy and zircon sand content between 2.5wt.% and 5wt.%. Although holding above the liquidus temperature up to 800 ºC and the use of zircon sand content of 5wt.% increases the viscosity of the melt alloy, the stability of the bubbles decreases. When holding temperature is increased from 800 ºC to 850 ºC, the use of zircon sand content of 5wt.% decreases the viscosity of the melt alloy. Hence the stability of the bubbles increases but the decrease in the content of zircon sand from 5wt.% to 2.5.wt.% increases the viscosity and the stability of the bubbles increases. These parameters use holding temperature, viscosity of melt alloy, content of reinforced materials influence the cell size and structure, which results in the variable mechanical properties.

Micro-hardness of the LM13 alloy composite foams material increases with an increase in the amount of reinforced zircon sand particles. However, 5wt.% zircon sand particles composite foam ($^{5}F_{800}$) shows maximum micro-hardness in comparison to other configuration of the composite foam at different phases.

Change in wear behavior of LM13 alloy foam was monitored with sliding distance at different loading conditions. It was observed that wear rate of all LM13 alloy foam increases with increasing applied load. A mild to severe transition in wear was observed at higher loading condition (5kg). Wear rate of the LM13 alloy composite foam was decreased with increasing amount of zircon sand particles in the melt matrix. However, 5wt.% zircon sand particles composite foam ($^{5}F_{850}$) shows poor wear resistance in comparison to the composites foam ($^{5}F_{800}$). This poor behavior against wear is observed due to the presence of larger cells in $^{5}F_{850}$ as compared to $^{5}F_{800}$. Decrement in wear rate of foam was observed with increasing reinforced amount in the alloy from 2.5wt.% ($^{2.5}F_{800}$) to 5wt.% ($^{5}F_{800}$) at same loads condition. After

analyzing all the data of LM13 alloy foam and composite foam, it was concluded that composite sample $^{5}F_{800}$ shows better wear resistance at different loads conditions in comparison to other developed LM13 alloy foam and composite foam.

5.2 Future Scope

The work done in present investigation has led to some conclusions which have been described in this work. However, the possibilities of further investigations of these developed LM13 alloy foams and LM13 alloy composite foams based on above work can be explored, some of which are as follows:

I. The developed LM13 alloy foams and LM13 alloy composite foams can be further investigated for their compressive strength, corrosion resistance along with some electrical and thermal measurement. It will help to widen their area of application in different engineering designs and applications.

II. The wear behavior of the LM13 alloy foams and LM13 alloy composite foams can be further analyzed at different environmental conditions like under lubricating condition and corrosive environment where temperature variability may be taken in to account.

III. Effect of heat treatment on wear properties of the foam can also be examined to have their wider applications.

IV. Apart from this, a new LM13 alloy foams and LM13 alloy composite foams of sandwich nature can be fabricated for different military applications. This particular type of structure will be useful in defence for following purposes.

- Porous aluminum foam material can be used as sound absorber in shooting range complex.
- In different parts of defence vehicles
- Beneath the vehicles to absorb shock waves
- To make safety box to carry different defence materials during warfare.